The effects of different levels of macronutrients on growth, histology and gene expression in the hindgut of Atlantic halibut (*Hippoglossus hippoglossus*)

Master of science in Biology- Aquaculture

Spring 2023

By Kristoffer Vestrheim

Supervisor: Dr. Øystein Sæle from The Institute of Marine Research

UNIVERSITY
OF BERGEN

The Department of Biological Sciences

University of Bergen, Norway

Table of contents

Acknowledgements

First of I would like to offer my gratitude to my supervisor Øystein Sæle from IMR for his knowledge and help during this process. I would also like to thank Senior engineer Hui-Shan Tung from IMR for her immense support and guidance in the laboratory with the RNA-work, which proved to be essential in completion of this thesis. I would also like to thank Head engineer Sarah Stoppel from IMR, for the assistance with the preparation of the histological samples. I am also very thankful to Even Fjære from IMR, for his involvement and time commitment during our conversations regarding many different topics surrounding this thesis.

I also want to thank my colleagues at Nordic Halibut for sharing their experiences and knowledge regarding halibut aquaculture. Lastly, I want to offer gratitude to my partner Marie Lynum, for supporting me and helping me deal with the journey that this last year has entailed.

Abstract

Atlantic halibut (*Hippglossus hippoglossus*) is the largest flatfish on earth, with a highly praised reputation as a food species. Due to the susceptibility for overfishing in the wild stocks, halibut aquaculture supplies the product demand that could not be met by fisheries alone. The largest bottleneck for the industry today is the slow growth of 4-5 years, where feed associated costs make profitability slow and cumbersome. The aim of this study was to study the effects of a mixed macronutrient gradient in 9mm pelleted feed, with different compositions of protein, lipids and carbohydrates in halibut growing from 300-1200g in a year. This was done to evaluate the effects on growth, while simultaneously evaluating fish health parameters using histological analysis and gene expression from the distal intestine. Results from this trial shows that the best growth was obtained in diets below 57% protein, with the best performance for a higher lipid content of up to 23%. A carbohydrate inclusion of 27% seemed to facilitate growth well, which could have huge implications for the potential of reduced feed-costs for producers. No dietary effect was observed in the distal intestine upon histological analysis. Furthermore, qPCR was carried out for the distal intestine, evaluating the expression of genes involved in inflammatory and mucosal responses. These include IL1b, IL6, IL11b, IL12b, IgM and imuc. Differences in expression showed an elevated response of IL1b and imuc associated with a higher inclusion of dietary lipids, with similar tendencies for higher carbohydrates.

Introduction

1.1. Norwegian halibut aquaculture

The Atlantic halibut (*Hippoglossus hippglossus*) is the largest flatfish on earth and can attain a weight of up to 300kg. It has a long history as an important species for Norwegian fishermen, and considerable quantities has been harvested since after World War 1 (Haug & Tjemsland, 1986). It has a high marked price and is regarded as a high-quality product due to most of the fish being fillet. Atlantic halibut is regarded as a stenohaline marine teleost, that experiences little fluctuations in salinity and temperature while in its natural habitat. It is adapted to a living in cold conditions with high salinity, which results in it having a slow growth and maturation (Haug, 1990). The Atlantic halibut has a high fecundity and is a batch spawner which spawns at depths from 300m-700m during the winter months in the North Atlantic fjords and coastal waters (Ottesen et al., 2009). A large female can have an egg production of up to 7 million eggs during one spawning season, which gives a great potential for recruitment (Haug & Gulliksen, 1988). The high fecundity of this fish comes at the cost of a less developed larvae. The high mortality in the early stages of life is a result of a reproductive strategy being based on great numbers, at the cost of a vulnerable early life stage with marginal chances of survival (Garrido et al., 2015).

The stocks of Atlantic halibut have proven to be very susceptible to overfishing, and because of this Norwegian stocks are strictly regulated (Haug & Tjemsland, 1986). This led to research and cultivation efforts during the 1980's, to develop an aquaculture industry to supply the demand that fisheries would not be able to meet (Mangor-Jensen et al., 1998). The expansion has since that time proven to be difficult, where slow growth and unreliable supply of fry has been two of the main reasons for the slow progress in the industry. These problems have for the part been solved by improvements in nutrition, rearing techniques, hygiene and genetics (Gallardo et al., 2022). In 2021 a total of 2716 tons of slaughtered halibut was sold from Norwegian farms, for 267 047 000 NOK (Fiskeridirektoratet, 2021). The preferred marked size for halibut is from 5-10kg, which normally takes about 4-5 years. This makes the production a long commitment, where high feeding costs makes profitability hard for the producers. This is seen as the biggest bottleneck today, where the slow grow-out phase in the open net-pens is expensive and delays profits many years after initial investments. Despite of this there is a lot of positivity around diversifying the Norwegian aquaculture industry, where halibut is seen as one of the most promising candidates by many (Mangor-Jensen et al., 1998).

1.2. Dietary composition

Halibut being a carnivorous marine species, it shares similarities to salmonids in the fact that it naturally adapted to diets high in marine protein and lipids. To replicate this diet commercially has a big impact on feed-cost, and for reasons concerning feed availability and sustainability a higher inclusion of plant-ingredients is desirable in the future (Egerton et al., 2020). Atlantic halibut (*Hippoglossus hippoglossus*) has shown no negative effects on growth when including soy protein concentrate (Berge et al., 1999). In addition no effect was found on either growth or intestinal morphology when including up to 36% full-fat soybean meal in fish with a starting weight of 169g (Grisdale-Helland et al., 2002). Replacing marine oils in commercial diets for halibut has shown promising results, where flaxseed oil and sunflower oil showed good digestibility in juvenile halibut (Martins et al., 2007). Other than this there is very little research done on plant derivatives being used in commercial diets for halibut.

Protein is the feed ingredient with the greatest economic impact on feed-costs. That is why the incentive is to give the halibut the lowest possible protein content, without negatively affecting growth (Aksnes et al., 1996). The way to do this is to change ratio between protein, lipid and carbohydrates in the feed. To do this, knowledge regarding minimum needs and upper tolerance levels needs to be established for the different macronutrients. Protein requirements has been found to decrease as the halibut grows, but there are some differences when it comes to the suggested minimum protein levels during the different stages (Árnason et al., 2009). Research on optimal macronutrient composition of feed for Atlantic halibut has mostly been done in juvenile fish. This is due to the critical stages of ontogeny and rapid growth that occurs during this stage, and where malnutrition has detrimental effects for the fish (Hamre et al., 2003).

After weaning unto a formulated diet halibut has shown a high protein demand, where levels from 58-63% of crude protein (CP) is suggested as a minimum from fish in the 0,4-6,5g range (Hamre et al., 2005; Hamre et al., 2003). For halibut from 7-500g a minimum of 630g kg^{-1} is suggested (Aksnes et al., 1996). In fish from 58g-126g the best growth was achieved in fish given the highest inclusion of CP in the trial which was 56% (Hatlen et al., 2005). This gives credibility to the notion that small juvenile halibut need a high inclusion of CP to support maximum SGR. Halibut growing from 140-260g showed no dietary effect on growth when varying CP content between 51-60% (Helland & Grisdale-Helland, 1998). For fish in the 559-877g range, research from 2009 found an increase in feed conversion rate (FCR) when going below 41% CP (Árnason et al., 2009). This is supported by results from a paper published in

2005, where they found no apparent effect in varying 41-56% CP in 800g fish (Hatlen et al., 2005). No minimum inclusion of protein has yet been determined for halibut over 1kg. When 35% CP was used as the lowest value for fish from 980-1493g, no effect was seen in going any higher (Árnason et al., 2009). This gives the indication of larger halibut having the opportunity of utilizing feed with a lower protein content than currently used, without compromising growth.

For carbohydrates a high sensitivity was found in juvenile fish from 0,4-6-5g body weight. Higher inclusions than 5% gave lower SGR, increased glycogen storage in the liver and higher hepatosomatic indexes ((Hamre et al., 2003). An increase in dietary starch from 7-10% in fish with a starting weight of 140g did not affect the fish in growth or hepatosomatic index (Helland & Grisdale-Helland, 1998). When comparing groups of 60g with 800g halibut an increase in carbohydrates only affected the 60g group negatively, where liver glycogen increased while SGR was lower (Hatlen et al., 2005). No effect of increased starch was observed in fish from 559-1493g in regards to SGR or HSI (Árnason et al., 2009). The dietary sensitivity to carbohydrates thus seems to be apparent in smaller fish, where bigger fish seem to tolerate a large range of dietary starch included in the diet.

There seems to be a generally large range of tolerability for lipids in halibut, but where weaning diets is recommended to be within the range of 5-30% lipid inclusion (Hamre et al., 2005). For halibut from 0,4-7g there was an increase in SGR with higher lipid, but no observed effect for the largest half of the trial. An increase of hepatocellular vacuolization in the liver, seemed to be a result of the higher inclusion of lipids (Hamre et al., 2005). In larger fish no apparent effect on growth has yet been seen in trials as of varying lipid-content (Aksnes et al., 1996; Helland & Grisdale-Helland, 1998; Nortvedt, 1997). The consensus is therefore that similarly to carbohydrates, larger fish seems to tolerate higher lipid-levels better compared to juvenile fish. In contrast there seems to be an observed effect on whole body lipid content increasing with higher lipid levels, and that slaughter quality and fillet composition might change according to the dietary lipid levels (Aksnes et al., 1996; Helland & Grisdale-Helland, 1998).

1.3. Immunological and GI response to feed ingredients

Immunological and inflammatory responses is an important aspect when assessing fish health and performance. Infections due to virus and bacteria is often the area that has the most detrimental effects on the host organism, but other causes can trigger inflammatory responses within the fish as well. The gastrointestinal tract is an important border between the inside of

the fish and the external environment, where its structural integrity represents a vital proxy of intestinal health (Chen et al., 2015). Research has proved that the posterior part of the gut in teleost fish contains several different immunological cell types, and is highly involved in response to pathogens (Yu et al., 2020).

The effect of antinutritional factors increasing following a larger inclusion of plant ingredients has been well described in several marine carnivorous fish such as Atlantic salmon (*Salmo salar*), Rainbow trout (*Oncorhynchus mykiss*) and Gilthead seabream (*Sparus aurata)* (Estruch et al., 2018; Sahlmann et al., 2013). Inflammation in the distal intestine of Atlantic salmon (*Salmo salar*) due to soybean products in the feed, showed an increase in susceptibility to disease for the host (Krogdahl et al., 2000). Evaluating the effect of different levels of single ingredients in feed is important to improve fish health and growth. Research on Atlantic halibut (*Hippoglossus hippglossus*) has shown no histological changes due to soybean inclusion in the feed, which might indicate that it is less sensitive to intestinal inflammation compared to salmon (Grisdale-Helland et al., 2002; Murray et al., 2010).

Comparing the intestinal response of changing macronutrient levels in the feed, might also reveal what composition facilitates for better performance and nutrient absorption. The morphological signs of inflammation in the distal intestine include shortening of the mucosal folds, smaller amounts of supranuclear vacuoles in enterocytes, a widening of the lamina propria in addition to increased leucocyte infiltration (Baeverfjord & Krogdahl, 1996). Thinner villi are also a common trait associated with gut-inflammation, where it can impact nutrient absorption capacity (Estruch et al., 2018). The sub-acute responses to gut-inflammation are recognized by reduced nutrient utilization and growth, combined with diarrhea as seen in Atlantic salmon (*Salmo salar)* and Rainbow trout (*Oncorhynchus mykiss*) (Baeverfjord & Krogdahl, 1996).

Interleukins are a group of cytokines which plays an important role in the intercellular regulatory processes of the immune system of fish (Secombes et al., 2011). These cytokines are produced in several cell types, but macrophages, endothelial cells and CD4+ T-helper cells being among the most important ones. The expression of these molecules is highly associated to both adaptive and innate immune responses, where many promote cascade reactions leading to inflammation (Øvergård et al., 2012). Measuring the expression of genetic markers associated with inflammatory responses in the distal intestine, is an important tool for giving a proxy for overall fish health and nutritional status as a response to feed composition.

1.4. Aims

The aim of this thesis was to study the effect of a different gradient of macronutrient in 12 diets using 9mm extruded pellets for Atlantic halibut, growing in separate tanks from 300g-1200g in one year. The aim was to include growth and performance metrics, combined with histological examination and gene expression analysis of inflammatory markers assessing intestinal health. By assessing the nutritional response of these diets, the aim was to study the tolerance of each macronutrient, and which macronutrient ratios yielded the best performance.

Material and methods

2.1. Feed production

The production of the feed used in this trial was led by Katerina Kousoulaki from Nofima, with Øystein Sæle and Eystein Overland participating from IMR. The selection of ingredients took availability for the industry into consideration and was otherwise chosen from an aspect of sustainability and quality. Having vegetables as a part of the diet was wanted, due to the positive impact from a sustainability aspect as well as reducing costs from marine ingredients. All the feed contained yttrium as marker to be used to measure digestibility. 9mm extruded pellets was conducted during the whole trial. A complete ingredients list is included in Appendix 1.

12 types of feed were produced for this experiment, which all have a different amount of protein, carbohydrates and lipids (Figure 1). The experimental design utilizes a triangular mixed design model, where the three macronutrients are compared in different concentrations in relation to each other. This equates to each macronutrient being found at 4 similar concentrations, all in differing mixing ratios. This gives statistical strength for the data and eliminates the need of replicates in the trial (Cornell, 2011)

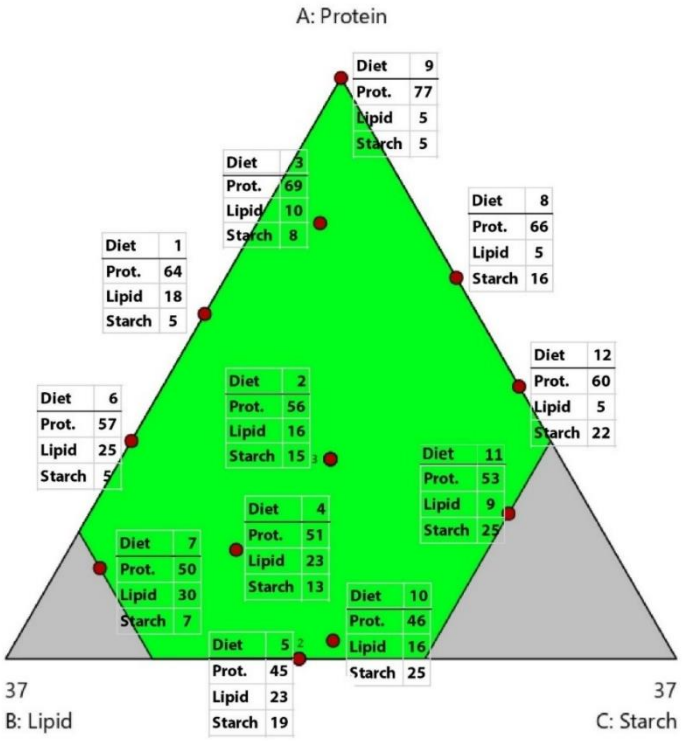

Figure 1. Macronutrient composition of the 12 diets used in the trial, where red dots correspond to the specific location in the triangular mixed design model. Values being closer to point A (Protein), Point B (Lipid) and point C (Starch) having an increased concentration of the given macronutrient.

2.2. Fish characteristics and experimental conditions

All the fish in the trial originated from Sterling white halibut. The fish were distributed into 18 separate tanks, with a diameter of 2,5 meters. Each tank originally contained 120 Atlantic Halibut (*Hippoglossus hippoglossus*), with an average weight of 300g. Each tank had a feeding automat, which operated from 08:00-18:00 every day. Each tank got the same amount of feed and followed a natural light-regime through the whole experiment (Astor ur). From the start the tanks had a flow rate of 3000 L/h, which was increased to 4000 L/h as the fish grew. Raw water from the sea holding a temperature of 8°C was used during the whole year. The fish were to stay in the tanks until they had reached an average weight of 1300g, which was estimated to happen after 1 year of growth. The growth was measured 5 times during the trial period, while simultaneously looking for outer health parameters such as wounds, fin and eye damage.

2.3. Measurement and weighing

Growth measurements were conducted by the following procedure during the experiment. Test fish were transferred from clean seawater, into anesthetizing tanks containing 20g/L of Finquel. Sedation normally occurred after 2-3 minutes of exposure. When the fish were sedated the PIT tag was read, and length (cm) and weight (g) was measured. The test fish were then moved back into the rearing tanks, where the level of oxygen was kept at 80-100%. The tanks were cleaned every time the fish were removed to be measured and weighed. For the final weighing after trial end, weight registrations for fish in tanks 8 and 6 were missing in the data sheet. This made 26 and 31 individuals the amount of weight registrations for tank 8 and 6 respectively.

2.4. Sample withdrawal

To be able to assess the changes during the experiment, an intermediate sample collection was conducted halfway during the trial. This was originally going to provide the results and basis of this thesis, where histology and gene expression after 6 months of feed exposure was to be analyzed. This was done the 25th and 26th of April 2022 at the IMR station in Austevoll. From each of the 18 tanks 6 halibut were chosen randomly and anesthetized. Measurements of weight and length was carried out after sedation. Blood samples from the posterior dorsal aorta was conducted, before the head was cut off. The abdominal cavity was opened, and clamps were put between the foregut, midgut and hindgut to minimize leakage between the different parts of the intestine. The foregut was then removed, and the content was put into

individual containers. The same procedure was repeated for the midgut, and then for the hindgut respectively.

Tissue samples for histological examination was then prepared for each of the three parts of the intestine. This was done by cutting the intestine using a pair of scissors to expose the inside. Then a tissue sample was taken by cutting the intestine vertically using a scalpel. The tissue sample was then rinsed in PBS. The tissue sample was then placed in an Eppendorf tube, containing formalin. For the hindgut an additional tissue sample was collected for RNA isolation, to assess gene expression in the tissue. This was rinsed in PBS as well, before it was placed in RNAlater. The tissue size being placed in RNA later was about 0,5cm in at least one dimension to minimize RNA degeneration. After fixation the formalin in the Eppendorf tubes were replaced with 70% ethanol before it was stored at -18℃ until further processing.

The end point sample collection occurred on the 7th and 8th of November 2022. An increase from 6 to 8 fish from each tank was agreed during this sampling, due to the observed discrepancy in growth between individuals from each group. Tank 10 which corresponds to samples from 73-80 was left out of this sampling, since the fish had already been slaughtered due to almost no growth in the tank. This was done from a fish welfare perspective, where it was no longer justifiable to keep the group in the experiment. The rest of the procedure was kept equal compared to the first sampling.

2.5. Histology

Histology sections of the hindgut was created using a Technovit 7100 kit for embedding the sections in resin and making microsections with a Histoknife device. The Technovit 7100 uses a hydrophilic resin based on 2-hydroxyethyl methacrylate, and Teflon forms which allows for a low polymerization temperature (20℃). This enables equal hardening of the block and facilitates for precise histological cuts and analyzation under a light microscope.

First part of the purification process was done on the 29th of September. Two rounds of a gradual concentration increase of rectified ethanol was conducted in the Eppendorf tubes in all the samples, first in 80% alcohol solution and 20% distilled water. After 2 hours all the liquid was replaced by pure rectified ethanol for 2 hours. A mix of 50% ethanol and 50% Technovit 7100 solution for pre-infiltration was then put on the tubes. The rest of the embedding was done according to the user manual of the Technovit 7100 kit. The samples were placed in preparation solution which was a mix of 100ml Technovit 7100 solution and 1g of hardener I. This was carried out in the Eppendorf tubes as previously, where the

solution covered the histological samples completely. The solution was mixed in an Erlenmeyer flask, with an IKA RCT basic magnetic stirrer with a magnet in the flask. After approximately 2h of mixing the powder in the solution was dissolved.

After infiltration the hindgut samples were cut individually with the use of a scalpel, to make smaller pieces fit for embedding. A smaller middle piece was cut horizontally on each sample, which gave a cross section of the distal intestine (Figure 2). The pieces were then placed in the embedding mold called Histoform, which had 9 slots for embedding. The molds were marked, and 6 hindgut samples were fit in each slot (Figure 3). Small plastic lids from a booklet were cut, to fit the top of the embedding molds to facilitate proper hardening. The pieces were placed on the side, which gives a cross section through the intestinal tissue. The first preparation solution was then mixed in a 15ml and 1ml hardener II relationship in a disposable plastic tube, where the new solution was given a good shake to ensure proper mixing. With the use of a pipette the embedding solution was placed carefully in the embedding mold containing the 6 pieces of hindgut samples, until it filled the mold up to the meniscus. The histology samples were then adjusted with the help a pair of tweezers, to strive for correct placement. This proved to be difficult due to balancing issues of the individual pieces, combined with a solution that hardens quickly. The plastic lid was then placed on top of the molds, where they were left in place to harden for approximately 48 hours.

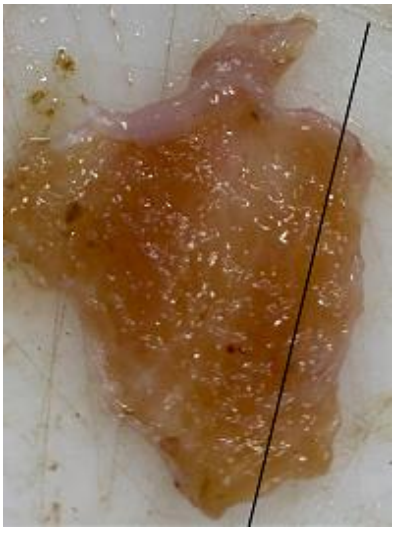

Figure 2. Distal intestine after being opened with scissors before being cut longitudinally, rinsed in PBS and placed in formalin. Photo: Kristoffer Vestrheim

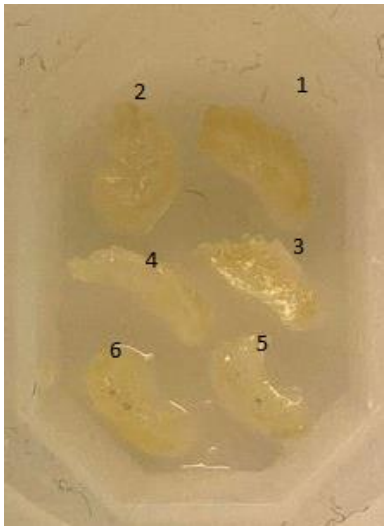

Figure 3. Cut, dehydrated and fixated hindgut samples. Fish 1-6 from each tank was fit into individual molds and placed on the side giving a cross-section of the inside intestinal surface. Photo: Kristoffer Vestrheim

After hardening the plastic lids were removed, and caps were mounted and glued with the use of Technovit 3040 yellow powder (Cold curing resin for surface testing and impression). The powder was mixed in a plastic weighing cup, where Technovit universal liquid was added until the liquid had a thick but runny consistency. The liquid was then poured on top of the embedding molds until it covered the surface. Caps for mounting the resin in the Histoknife machine were then glued on top, and backsides marked for correct orientation.

After the glue had hardened, the resin was removed from the mold and marked with a cut in the right corner for orientation. A Leica RM2255 microtome was used for cutting, with carbide metal blades. Sections of 3 µm were made and placed on a glass slide (SuperFrost ®, Menzelglaser, Germany).

The sections were then dried on a heating table for over 10 minutes at 75 °C. Toluidine blue was used to stain the samples. The stock solution was made with 1g of Toluidine blue, 1g of Borax and 100ml of ddH20. After mixing and filtering, some of the stock was diluted with ddH20 in a 1:10 ratio. The slides were submerged for a few minutes each in the diluted solution and rinsed of in running water. After drying, cover glasses were glued onto the slides and left overnight until the xylene had evaporated in an extractor hood.

After analyzing the colored slides in a light microscope, it turned out that all the histological sections had varying degrees of cell damage (Figure 4). This was speculated to be because of the formalin not working as intended, where the cell damage did not resemble uncareful handling but rather un-fixated tissue. It could be due to the formalin containing something else, or potentially something being wrong with the batch. This has not been confirmed as the formalin has been disposed of. This resulted in having to redo the histology, using the data collected from the end point sampling instead. The procedure was kept the same as for the previous sampling and was started the 5th of January 2023. Head engineer Sarah Stoppel from IMR assisted with the microtome cutting and staining.

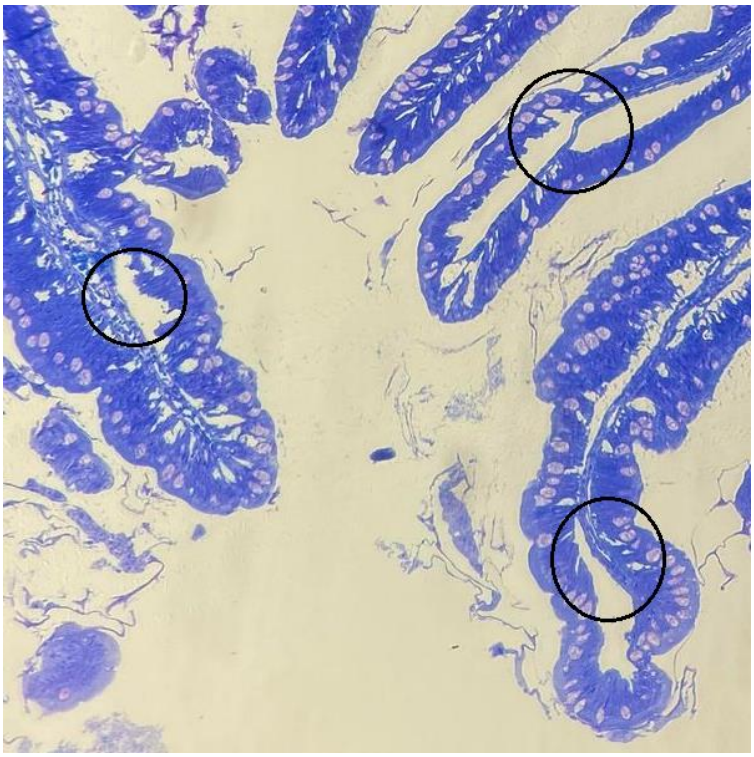

Figure 4. Microscopy using a light microscope on x40 magnification, with resin fixated hindgut samples from Atlantic halibut (Hippoglossus hippoglossus) stained with toluidine. Histology cross section from tank 10 in the intermediate sampling from April 25th and 26th 2022, showing cellular damage highlighted by the black circles. All samples from the intermediate sampling showed varying degrees of cellular damage and was therefore replaced by samples from the end point sample collection on the 7th and 8th of November 2022.

2.5.1. Microscopy

The images for each slide were photographed using 40x magnification. The evaluation system used in the microscopy part consisted of a quantitative and semi quantitative image analysis. This scoring system was developed and derived from previous image analysis systems used for evaluating enteritis and inflammatory responses in salmon (Bakke-McKellep et al., 2007; Nimalan et al., 2022; Silva et al., 2015), which also has been done in halibut before (Murray et al., 2010). The quantitative part was based on measuring villus height (VH) and villus width (VW), which is shown in Figure 5. Each villus was measured 5 times using the ImageJ extension in Qupath, and the average for each sample was registered (Bankhead et al., 2017). A scoring system (Table 1) from 1-5 was developed for the number of mucus cells (NM) and Lamina propria appearance (LP).

Table 1. Scoring system for mucus cells evaluation and lamina propria appearance, where each sample is given a score from 1-5.

NM	
1	Above 31 mucus cells per villus, densely distributed and small
2	26-31 mucus cells per villus, both small and large
3	21-26 mucus cells, many small and few large
4	16-21 mucus cells, few small and many large
5	Bellow 16 mucus cells, large and evenly distributed
Lamina propria	
1	Lamina propria is very thin
2	Lamina propria appears more distinct in some folds
3	Lamina propria is more distinct in most folds
4	Lamina propria is thick in many folds
5	Lamina propria is very thick in many folds

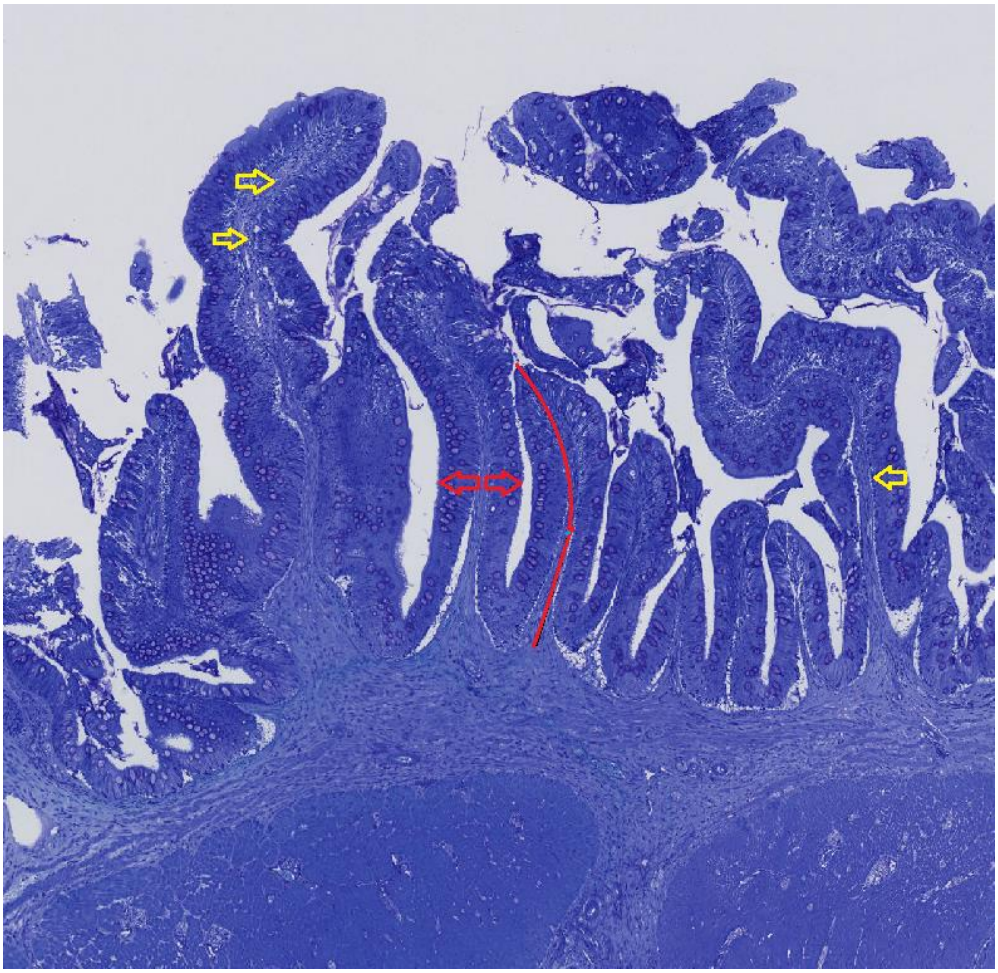

Figure 5. Image of intestinal folds of Atlantic halibut in Qupath software. Yellow arrows showing the lamina propria, red arrows showing the width of the individual villus and the red line showing the villus length.

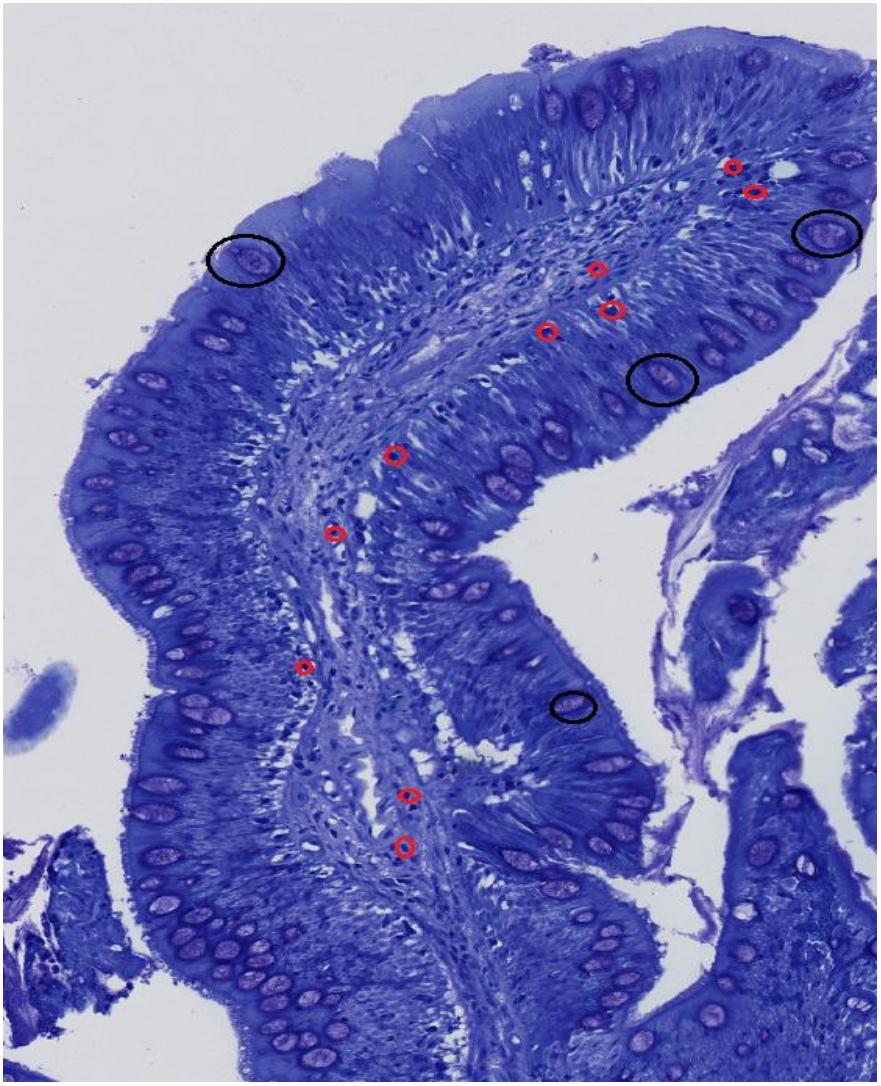

Figure 6. Intestinal fold of Atlantic halibut. Black circles showcasing mucus cells, and red circles showing leukocytes in the lamina propria.

2.7. Gene expression

The analysis of gene expression was carried out at IMR Nordnes. Because of the hindgut samples being used in histology was discarded due to cellular damage, the gene expression analysis was carried out on the end point sample collection similarly to histology. RNA was extracted from the hindgut using EZ1 and treated with DNase to remove possible DNA contamination. Then cDNA was synthesized using RNA and reverse transcriptase. The relative gene expression of target genes was measured and compared to stable control genes with qPCR. All work with solvents was carried out in the fume hood in the molecular lab at Nordnesboder, where the rest of the gene expression work was done as well. The procedure was done according to instructions of the manufacturer, with guidance from senior engineer Hui-Shan Tung at IMR.

2.7.1. RNA extraction

RNA extraction was done using a EZ1 RNA Tissue Mini Kit. The samples had been placed on RNA later and stored in a freezer holding -22 ℃. A small piece of tissue was cut with a scalpel and placed in precellys tubes for homogenizing. Qiazol which is a monophase solution containing guanidinium salts and phenol was added to the tubes for homogenizing. Chloroform for separating RNA from proteins and DNA was added after, where the RNA binds to the magnetic adhesive particles and can be washed and eluted in H2O. To remove DNA traces causing contamination, DNase treatment was used as well. The RNA concentration was measured using spectrophotometry in Nanodrop (Thermo Scientific, Waltham, Massachusetts US). Nanodrop is a spectrophotometer which measures absorbance. The absorbance-ratio of 260nm to 280nm gives an indication of concentration of RNA compared to leftovers of DNA, protein and phenol. This is used as a tool to measure purity of RNA. The absorbance of 260nm to 230nm is used to determine the contamination of salts present in the samples, which can inhibit the downstream analysis in the qPCR. The preferred ratio of 260/280 is 1.8-2.1, and 260/230 is ≥ 1.7.

Samples were placed on ice 6 at a time to avoid unnecessary degradation, and due to the EZ1 robot taking a maximum of 6 samples at a time. 3-4 beads were added to precellys tubes with 750 µl of Qiazol. Tissue sizes were adjusted with a scalpel where needed, to the recommended size for intestine which is 100mg. The samples were put in the tubes and shaken for 10 seconds. Homogenization was carried out a precellys 24 homogenizer at 6000rpm for 3 x 10s, before incubating 5 minutes in room temperature (RT). 150 µl chloroform was added to the tubes and shaken for 15s and then incubated for 3 minutes RT. Samples were then centrifuged for 15 minutes at 12 000 x g at 4 ℃ in an Eppendorf Centrifuge 5415R. The upper phase containing RNA was transferred to 2ml sample tubes.

DNase was put on ice, and the EZ1 robot and piercing units cleaned with H2O and 70% EtOH. Reagent Cartridges were shaken and put into the EZ1 racks and 10 µl of DNase added to well 5. Holders and tips were placed in the second and third row in the EZ1 metal rack, 1,5ml Elution tubes in row 1 and 2ml sample tubes in row 4. Total RNA for universal tissue including DNase in 100 µl elution was the selected protocol running for 45 minutes. The samples were frozen in a -80℃ freezer until measuring purity in nanodrop and registered in LIMS.

A portion of the samples proved to have low concentrations and unfavorable 260/280 and/or 260/230 ratios. The absorbance was speculated to be due to the beads in homogenization not being cleaned well enough after use and causing salt contaminants. After using clean beads in the hominization, the absorbance improved somewhat, but some of the samples still appeared to have unfavorable ratios further down the extraction. In the first 2 rounds of the extraction corresponding to samples 1-12, tubes in row 1 were mistakenly put in the freezer coming out of the EZ1 machine instead of tubes from row 4. Not having more tissue samples of these unfortunately caused these samples to be left out from further analysis.

Quality and degradation were examined using Agilent 2100 Bioanalyzer using the Agilent RNA 6000 Nano kit. The analysis was done according to the instructions of the manufacturer. 550 µL of RNA gel matrix was pipetted into a spin filter and centrifuged at 1500 x g for 10 minutes at room temperature. 1 µL of RNA dye concentrate was vortexed and added to 65 µl of the filtered gel. Then the mix was vortexed and centrifuged at 13000 x g for 10 min at RT. The ladder and samples got heat denatured at 70 °C and then immediately cooled on ice. A selection of samples was chosen semi randomly, where the lowest concentrations from nanodrop was left out. 9 µL gel-dye mix was pipetted into well 3 in the 4th column of the RNA chip. The plunger was set to 1 ml and pressed down until the clip held it. The clip got released after 30 seconds and the plunge pulled back to the initial position after about 5 seconds. The prime station was opened and 9 µL of gel-dye mix pipetted into well 1 and 2 of column 4. 5 µl of RNA marker was added to the ladder well and 12 sample wells. For the ladder well 1 µL of RNA ladder was added in column 4. Then 1 µL of every sample was pipetted into each of the 12 sample wells. The chip was placed horizontally in an ICA vortex mixer and vortexed for 60 seconds at 2400 rpm. The samples were then analyzed in the Agilent 2100 Bioanalyzer machine, with Eukaryote Total RNA Nano being the selected program. The RNA integrity number (RIN) was analyzed, and mRNA peaks checked after the run was complete.

2.8. CDNA

Complementary DNA is synthesized with the use of RNA as a template. The enzyme Reverse Transcriptase was used to form cDNA, which is complementary to the RNA. This stable form of RNA is a representation of the active genes in expressed in the intestinal cells during the moment of sampling. A 30 µl reaction was chosen, due to the number of genes being run was less than 25. Because of some samples showed low concentrations (< 50ng/µl), a starting concentration of 25ng/µl was chosen, and dilution curve adjusted accordingly. All samples

were diluted with ddh20 individually in a new set of tubes. RNase free water was taken from the milli-q and added to the tubes first, before RNA was added from the RNA samples. Concentration was then measured again in nanodrop and adjusted until concentration was within 5% of 25ng/µl.

A pool of RNA samples was made by taking 10 µl from sample 17, 22, 24,36,37,42,43,51,54,58,70,82,84,86,90,91,93,94,98,100,101,102,107, 110 and 30 µl from 92. The samples were chosen semi randomly, where low concentrations were left out to ensure the concentration being high enough for 4 plates of cDNA without taking too much out of the original samples. The concentration of the pool measured to be 273 ng/µl. The dilution curve was prepared by adding 73,5µl ddh20 and 16,5 µl of RNA from the pool into tube A, giving 90 µl of 50ng/µl. 45 µl of ddH2O was added in tube B-F. The concentration was then measured to be within 5% in nanodrop or adjusted accordingly. 45 µl was then added from tube A into B and concentration measured but not adjusted. Tube B was then mixed and transferred 45µl to tube C, as was done until tube F.

The samples and standard curve were run in triplicates in the cDNA plate, to better distinguish possible outliers for each sample. The reaction mix that had been thawed on ice before mixing (Table 1) was added to all the wells except for the two negative controls. One being a nonamplification (NAC) and no template control (NTC) occupying the last two wells respectively. The NAC well was added 20 µl of reaction mix before the enzymes were added. After adding the multiscribe enzyme and RNase inhibitor the tube was carefully inverted 6 times. 20 µl of the mix was then added to all the wells excluding NAC. 10 µl the dilution curve from A was added to the first 3 wells with the use of a 10µl pipette, as well as 10 µl from dilution curve A to NAC control. The rest of the dilution curve was added in triplicates in order, before including 10 µl from the RNA samples individually in the rest of the wells. Lastly 10 µl of ddH20 was added to the NTC well. Each plate having 96 wells corresponds to taking a maximum of 25 samples when excluding the controls and dilution curves, which resulted in 4 cDNA plates being made.

Table 2, reagents used in the creation of each cDNA plate for a 30 µl reaction.

Reagent (not enzymatic)	**30 µl reaction**
ddH2O	130 µl
10x TaqMan RT buffer	300 µl
25 mM $MgCl_2$	660 µl
10mM deoxyNTPs Mix	600 µl
50 µM oligo $d(T)_{16}$ /Random hexamers/	150 µl
Reagent (Enzymes)	
RNase Inhibitor (20U/µl)	60 µl
Multiscribe Reverse Transcriptase (50U/ µl)	100 µl

The cleaned well plate cover was added to the top of the plate, before centrifuging the plate at 50 x g for 60 seconds. The cDNA synthesis was done using a Bio-Rad T100 Thermal cycler and choosing a 30µl reaction. The instrument setup was set to 10min of 25℃ for activation, 60min of 48℃ reverse transcription (RT) and 5 minutes of RT inactivation at 95℃. The plate was held at 4℃ in the machine, until it was centrifuged at 1200 x g for 60 seconds. The plate cover was then removed, and tape pad added before it was stored at -20℃ until qPCR.

2.9. Target genes and primers

Standard genes relating to cytokine and intestinal inflammatory responses to feed, seen in several fish species was chosen (Estruch et al., 2018; Øvergård et al., 2012). Interleukin 1b, IL6, IL11b and IL12b has been characterized in Atlantic halibut (*Hippoglossus hippoglossus*) (Øvergård et al., 2012), which were the genes relating cytokine activity chosen for gene expression analysis. IgM relating to prolonged immune reactions from specific antibodies was also included (Wilson & Warr, 1992). Intestinal mucin (imuc) relating to intestinal epithelial protection was included, where its expression is highly dependent on the nutritional status as seen in Gilthead seabream (*Sparus aurata)* in previous research (Pérez-Sánchez et al., 2013). Elongation factor 1 alpha (EF1A1) and β-actin was chosen as housekeeping genes, as they have showed stable expression in Atlantic halibut (*Hippoglossus hippglossus)* tissues (Øvergård et al., 2010).

The specific gene locations were found using the national library of medicine (NCBI) databases with Atlantic halibut (*Hippoglossus hippoglossus*) as the target organism. Then adding the gene name in the nucleotide search and choosing the “Primer BLAST” function for

the specific sequence. The PCR product size was selected to be within 70-200, where exon junction span was left as "no preference" due to RNA being treated with DNase. The rest of the settings were left as default.

Table 3. Primer sequences used in qPCR for gene expression analysis. Gene name, primer sequence, amplicon size and PCR efficiency are shown accordingly.

Gene	Sequence (5'→3')	Bp
IL1b	F1: ACCGCAGGGAGACAGGATTA R1: CTCCTGCTCATAGGAGGTGC	86
IL6	F1: GAAGGAGCACGTCAGGGAAA R1: ATTAAAGCCCTCAGGCCCAC	155
IL11b	F1: AAAACTCCGGAGACGGGAGA R1: ATCCTCTGAGCACAACGCAA	102
IL12b	F1: CTTCCCTGGTACCGAAGAGC R1: CGCACGTGAGAGGACCTTAT	192
IgM	F1: ATGGCTGAAAAATGACGCGG R1: CAGCATACTGGCCGCTTTTC	164
imuc	F1: CTGGAGGATCCACTCAGGC R1: AGAACCCTCGGAGCAGTTTG	155
EF1A1	F1: TGGAAAGACGACCAAGGCTG R1: GAAGATAGAGTGGCCCGCTG	108
β-actin	F1: CGGCATCCACGAGACAACT R1: GTATTTACGCTCAGGTGGGG	196

2.10. OneStep RT-PCR and gel-electrophoresis

Before running qPCR with the cDNA plates, the primers were tested with the OneStep RT-PCR kit and agarose-gel electrophoresis. Template RNA from the cDNA pool was used as template for cDNA synthesis and PCR in the same tube for each primer before being run in an agarose gel. This is a method of separating DNA fragments with different sizes with the use of an agarose-gel. With DNA having a negative charge, they will travel towards a positive electrical pole. This causes small fragments of DNA to travel further compared to larger ones. To detect the DNA GelRed Nucleic Acid Stain var used, which makes it visible under UV-light.

Firstly, the desalted primers were spun and diluted to 50µm with TE buffer before being vortexed for 15 seconds. Then a master mix of reagents was made (Table 2) and 25 µl pipetted into eight 0,2ml tubes. The specific primers were then added into the tubes separately. RT PCR reaction was then run on the Bio-Rad T100 Thermal cycler, using the

OneStep RT-PCR program which takes approximately 3 hours. The settings were RT for 30min at 50℃, PCR activation for 15min at 95℃, 3 step cycle, denaturation for 45s at 94℃, annealing for 45s at 60℃, extension for 1min at 72℃ and final extension for 10min at 72℃.

1g of agarose gel and 50ml of TAE buffer was mixed in a 250ml Erlend Meyer flask. The mix was heated in a microwave for about 1min until the agarose was dissolved in buffer, then taken out for about 15s before being slightly cooled down using running water on the outside of the flask. 5 µl of Gel Red was added to the 50ml of melted agarose-gel and mixed carefully. The agarose was then added to the cast, and the comb put in place before the gel was left for 30min to harden. 2 µl of 6x loading buffer was added to 10 µl of sample, which gives 12 µl which is about the same amount that the wells can take. The cast was then filled with ddH2O diluted TAE buffer (50:1 H20/TAE), and the gel placed in the cast. The comb was then removed and 12 µl of DNA ladder added to the first well, and 12 µl of sample added to the eight next wells. The lid and poles were put in place, and the machine turned on for about 30min at 84V. The gel was then analyzed in G-box with the GeneSys software (Syngene), and the picture saved (Figure 7).

Table 4, reagent amounts used for 225 µl reaction.

Reagents (Master mix)	**225 µl rxn**
5x QIAGEN One Step RT-PCR buffer	45 µl
Q solution	45 µl
dNTP mix	9 µl
RNase free H2O	100 µl
RNase inhibitor	2.25 µl
QIAGEN One Step RT-PCR Enzyme Mix	9 µl
Template RNA mix (273ng/µl)	13,5 µl
Spesific primers	
Primer forward	0,5µl
Primer reverse	0,5µl

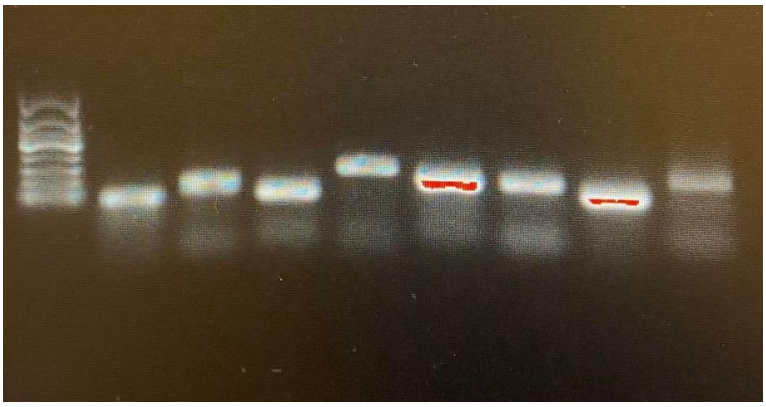

Figure 7. Agarose- gel electrophoresis for the 8 different primers using RNA pool as template. Ladder from the left and IL1b, IL6, IL11b, IL12b, Igm, imuc, EF1A1 and β-actin respectively. All samples showing product amplification. Photo: Kristoffer Vestrheim.

2.11. qPCR

To measure relative gene expression of the selected genes qPCR was conducted. The genes were compared to housekeeping genes, where amplification occurs to both the reference genes and the target genes. The amount of fluorescence increases relative to the amount of product being synthesized. This was done with the use of a SYBR Green reaction mix and using the cDNA plates as template. The qPCR was run in the C1000 Touch Thermal Cycler and analyzed using the Bio-Rad CFX Maestro software.

The cDNA plate and reagents were thawed on ice, and the plate centrifuged at 1200x g for 1 minute and then vortexed at 1500 rpm for 5 minutes. The qPCR plate consists of 386 wells, where 2 genes for 2 plates were synthesized each run. The reagents master mix was made in four 1.5 Eppendorf tubes, before 112µl from the mix was transferred to each well in an 8-strip tube. This was done for all the tubes with the different primers. The four 8-strip tubes were then pipetted by a Biomek 4000 pipetting robot into the 386-qPCR plate, using 8 µl of master-mix for each well. The robot then added 2 µl of cDNA from each well from the two cDNA plates. An optical adhesive cover was then added to the qPCR plate, before it was centrifuged for 2 minutes at 1500x g. The qPCR reaction in a final volume of 20 µl was started in the Bio-Rad T100 Thermal cycler, using the SYBR green program. The program starts with 5min of preincubation at 95℃, 45 amplification cycles at 95,60 and 72℃ for 10s respectively. Melting point analysis at 95℃ for 5s, then 65℃ for 1min, then 97℃ before cooling at 40℃ for 10 seconds. After the analysis the template was created in the CFX Maestro software corresponding to well setup. Unexpectedly Beta-actin showed low amplification in all wells, which left EL1A1 to be the only reference gene used.

Table 5, reagents in the SYBR-green reaction mix.

Reagents (Master mix)	**115 rnx**
Primer forward	11.5 µl
Primer reverse	11.5 µl
SYBR GREEN PCR Master Mix (2X)	575 µl
ddH20	322 µl

2.12. Calculations and statistics

The specific growth rate (SGR) which is the percentage increase in body weight per day, was calculated by the following formula:

$SGR = (\ln W_n - \ln W_0) / \Delta T \times 100$

W_n and W_0 being the weight at the end and start of the measurement period respectively, and ΔT being the number of days in between the two measurements.

The ANOVA for SGR, weight, histology and gene expression was done in Design-Expert v12 (Stat-ease). RStudio was used to make figures for gene expression and weight. The average SGR for each tank in measurement period was plotted into design expert, where the specific diet was represented as a point in the triangular mixed design model. This was represented by a color profile corresponding to the value, to better visualize changes in SGR between the different macronutrients. An ANOVA analysis was fitted to the model, where the model terms were deemed as significant at $P<0,05$.

Results

3.1. Growth

After the second measurements, tank 10 which was given the highest lipid inclusion (diet 7) was terminated due to poor performance and not included in Figure 10,13 or 14 showing SGR, or in Figure 8 and 9 showing final weight. The poorest performance from the end point was seen in diet 3 (675g) and 9 (765g) which were the diets given the highest inclusion of protein. The best performance was seen in diet 6 with an average weight of 1102g, followed by diet 5.1 and 5.2 with a combined average of 913g. Next was diet 11 and 10, which ended at 888g and 879g respectively. The ANOVA for the linear regression model for end point weight (Figure 10), deemed the model as not significant at a p-value of 0.1127 (Appendix 2). The best preforming diets looking at macronutrient composition, were diets below 57% in protein. Looking at the growth-distribution, lipids seemed to facilitate growth better than starch in this trial, except for the highest lipid content seen in diet 7. Diet 10 and 11 with the highest starch content (25%) were the third and fourth best preforming diets. A high degree of variation was seen within each population group, with large discrepancies of growth between the individuals.

The models for SGR (Figure 10,11,12,13 and 14) shows growth trends changing during the time period. In Figure 13 showing SGR4, diet 9,8 and 12 had the best growth. These diets were all high in protein and low in lipids. This model was deemed with a p-value of 0,0205. For SGR 1-3 (Figure 11,12,13) the diets having the highest final weight were consistent with best growth, with some dynamics changing during the different growth periods. The figure for total SGR (Figure 10) shows a pronounced effect on high lipid and low protein on better growth, with a p-value of 0,0112 for the ANOVA fitted to the model.

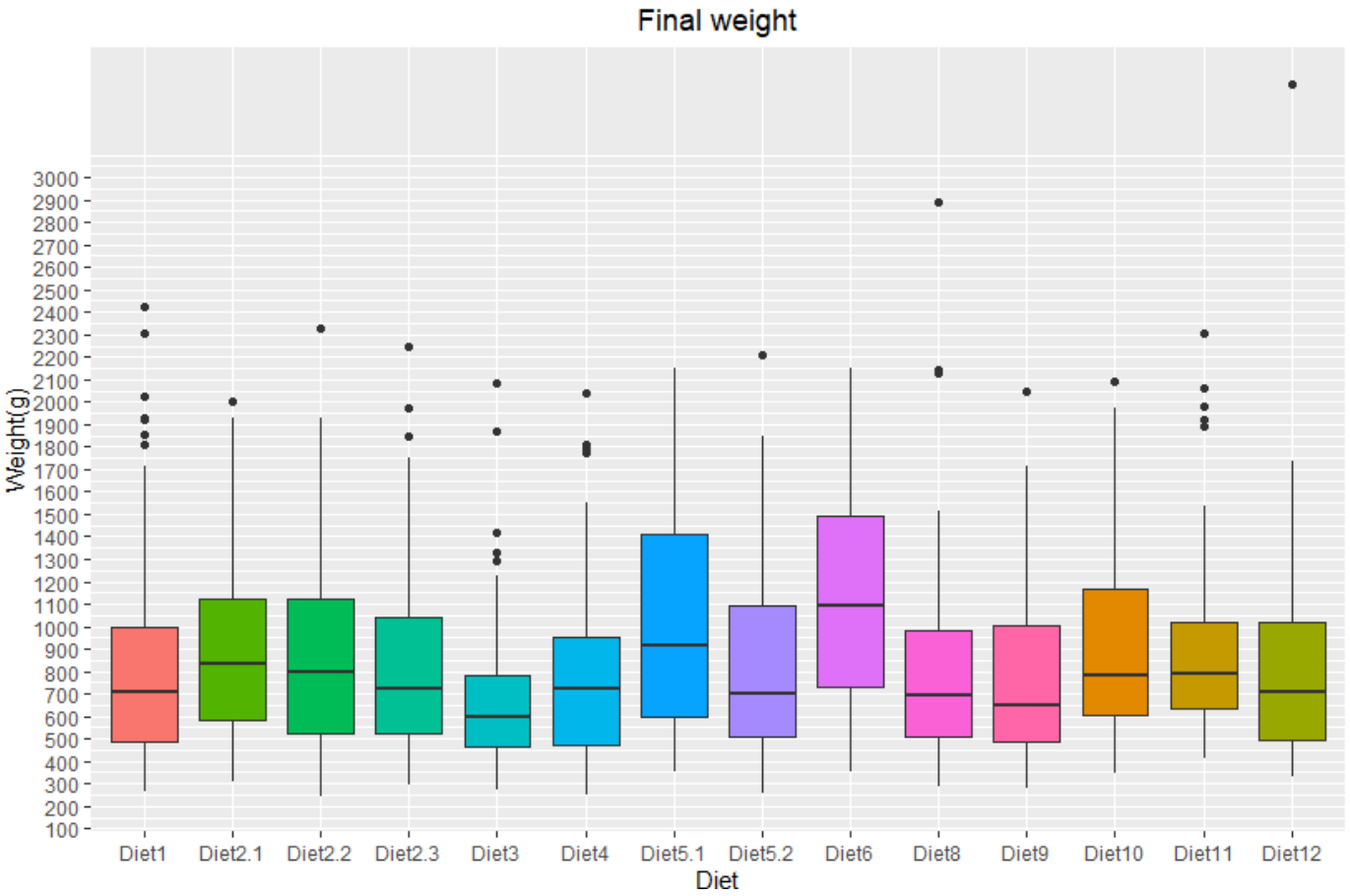

Figure 8. Final weight of Atlantic halibut from the end point sampling. Horizontal lines mark the mean, vertical lines mark the standard deviation, and dots marks the outliers. N=1176 fish in total.

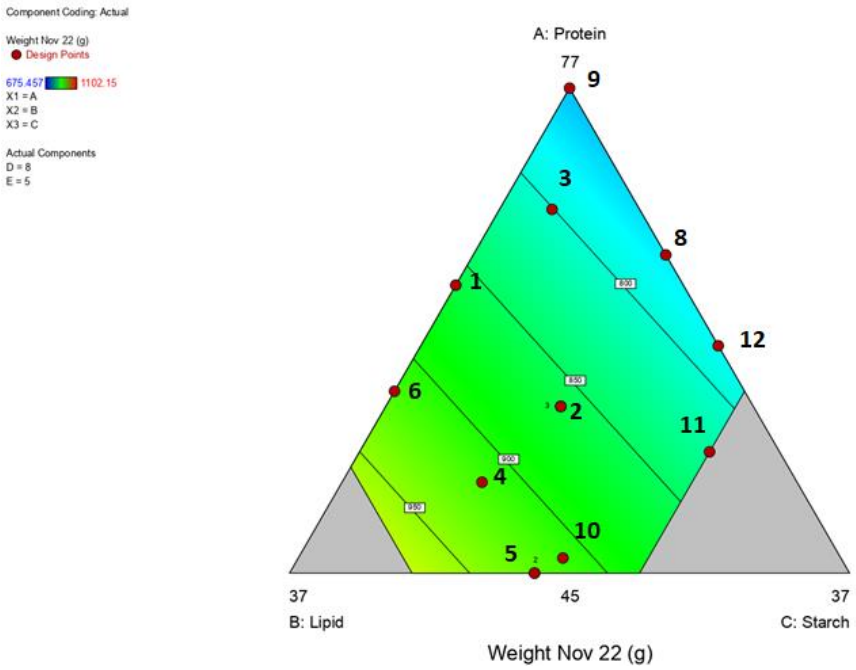

Figure 9. The mean final weight of Atlantic halibut from the end point sampling presented in a color spectrum, where blue is the lowest value and red being the highest. The specific macronutrient composition of the diets represents a red dot in the triangular mixed design model, where the positioning in relation to point A (Protein), point B (Lipid) and point C (Starch) corresponds to the macronutrient content of the given diet. N=1176 fish in total. P-value=0,113.

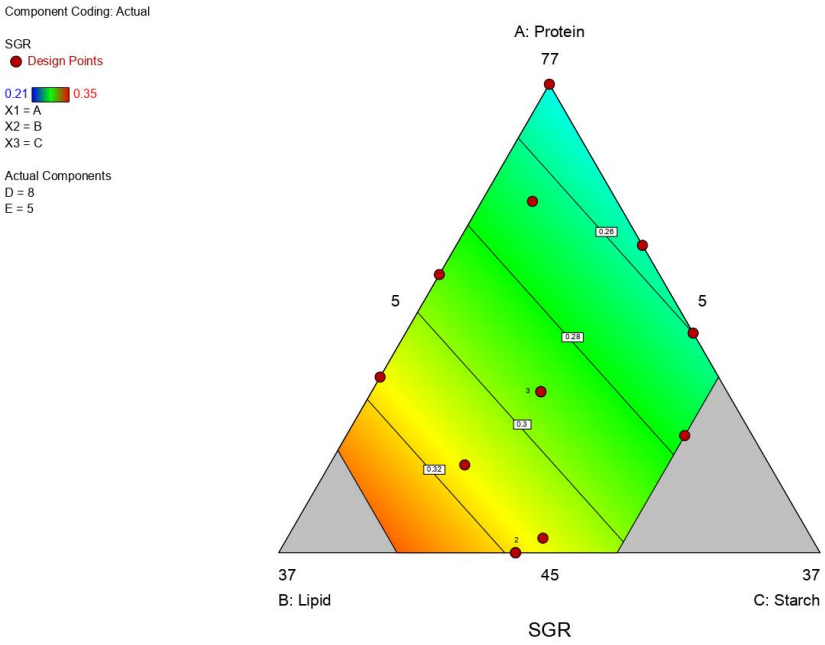

Figure 10. The specific growth rate of Atlantic halibut for the whole period. The measurements are presented in a color spectrum, where blue is the lowest value and red being the highest. The specific macronutrient composition of the diets represents a red dot in the triangular mixed design model, where the positioning in relation to point A (Protein), point B (Lipid) and point C (Starch) corresponds to the macronutrient content of the given diet. N=1176 fish in total. P-value=0,011.

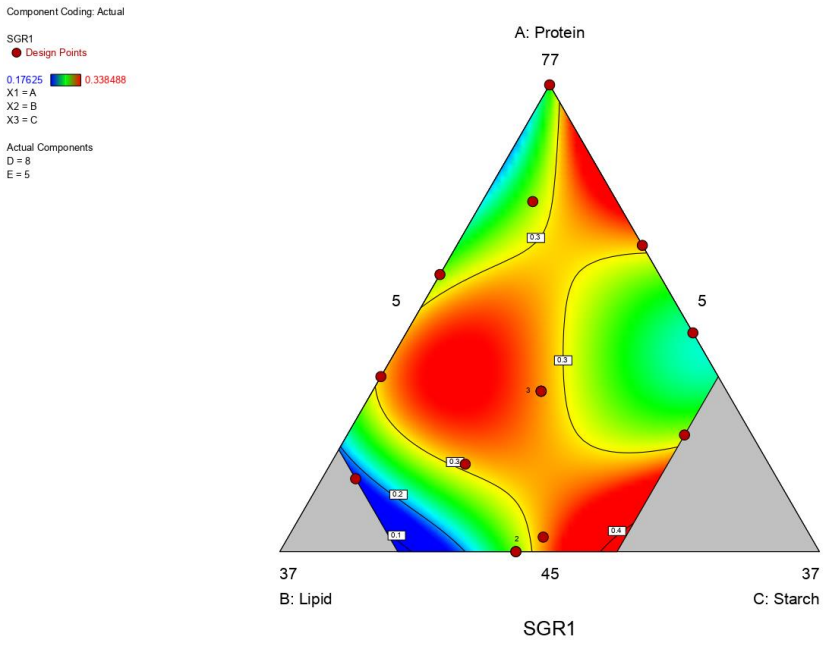

Figure 11. The specific growth rate of Atlantic halibut from the first measurement presented in a color spectrum, where blue is the lowest value and red being the highest. The specific macronutrient composition of the diets represents a red dot in the triangular mixed design model, where the positioning in relation to point A (Protein), point B (Lipid) and point C (Starch) corresponds to the macronutrient content of the given diet. N=1434 fish in total. P-value=0,046.

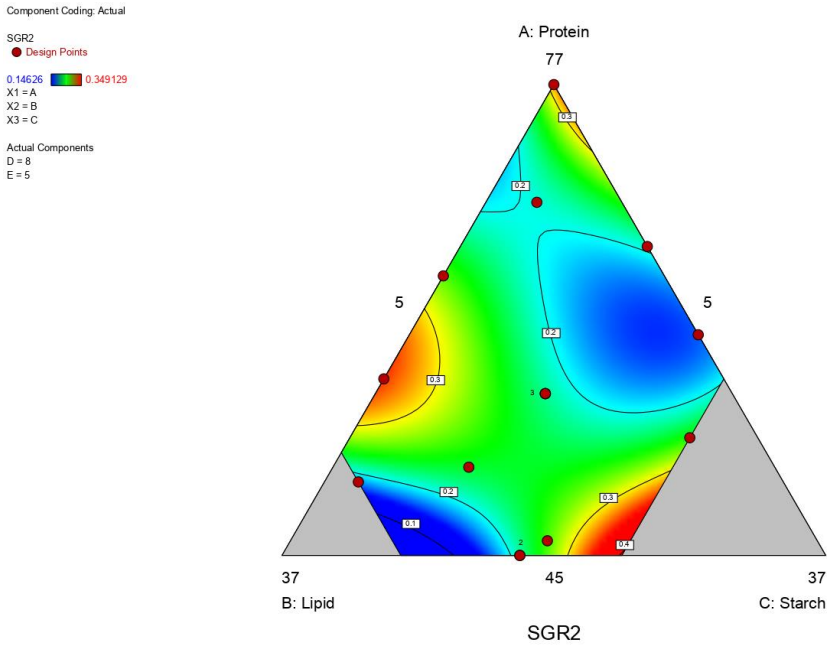

Figure 12. The specific growth rate of Atlantic halibut from the second measurement presented in a color spectrum, where blue is the lowest value and red being the highest. The specific macronutrient composition of the diets represents a red dot in the triangular mixed design model, where the positioning in relation to point A (Protein), point B (Lipid) and point C (Starch) corresponds to the macronutrient content of the given diet. N=1502 fish in total. P-value=0,458.

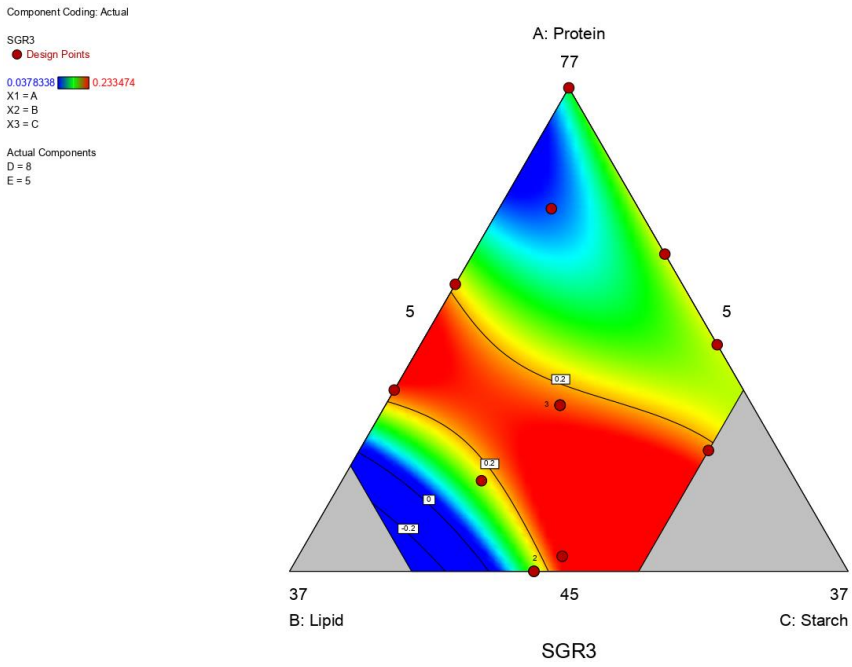

Figure 13. The specific growth rate of Atlantic halibut from the third measurement presented in a color spectrum, where blue is the lowest value and red being the highest. The specific macronutrient composition of the diets represents a red dot in the triangular mixed design model, where the positioning in relation to point A (Protein), point B (Lipid) and point C (Starch) corresponds to the macronutrient content of the given diet. N=1383 fish in total. P-value=0,071.

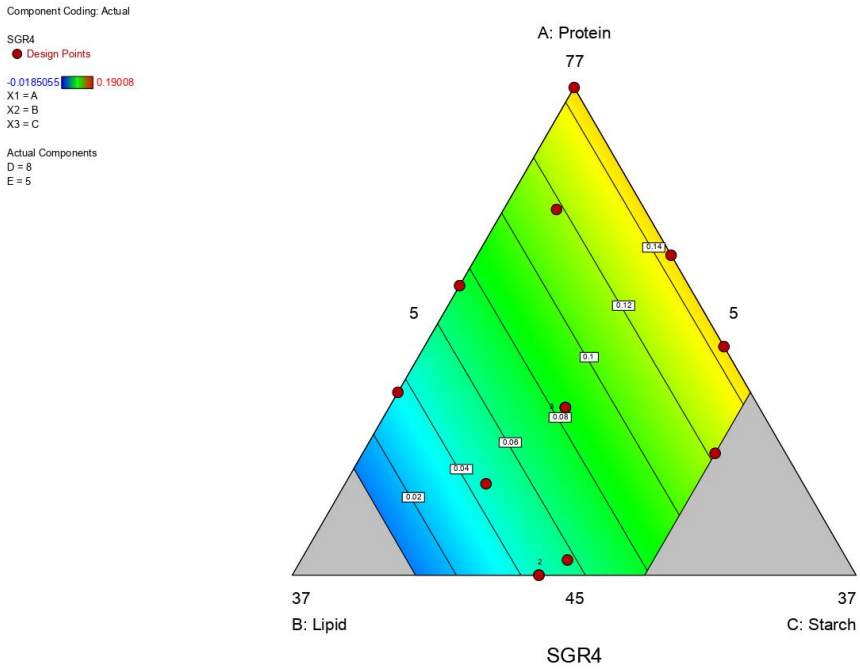

Figure 14. The specific growth rate of Atlantic halibut from the final measurement presented in a color spectrum, where blue is the lowest value and red being the highest. The specific macronutrient composition of the diets represents a red dot in the triangular mixed design model, where the positioning in relation to point A (Protein), point B (Lipid) and point C (Starch) corresponds to the macronutrient content of the given diet. N=1139 fish in total. P-value=0,021.

3.2. Histology

The sections showed a large variation of height and width between villus in the same sample, where cross section quality and visibility varied a lot as well. Large differences between villus from the same sample was seen, considering the lamina propria and mucus cells as well. No clear correlation between diet and histological evaluation was apparent, when plotting the values into the design model accounting for macronutrient composition (Figure 18,19,20 and 21). Villus height appeared shorter with higher lipids according to Figure 18, but the model deemed as not significant (p-value= 0,54). Villus width seen in Figure 19 (p-value= 0,446), shows villus being the widest towards the higher protein inclusion, as well a tendency with higher starch content. No macronutrient effect was seen on lamina propria appearance (Figure 20), or on goblet cell composition (Figure 21).

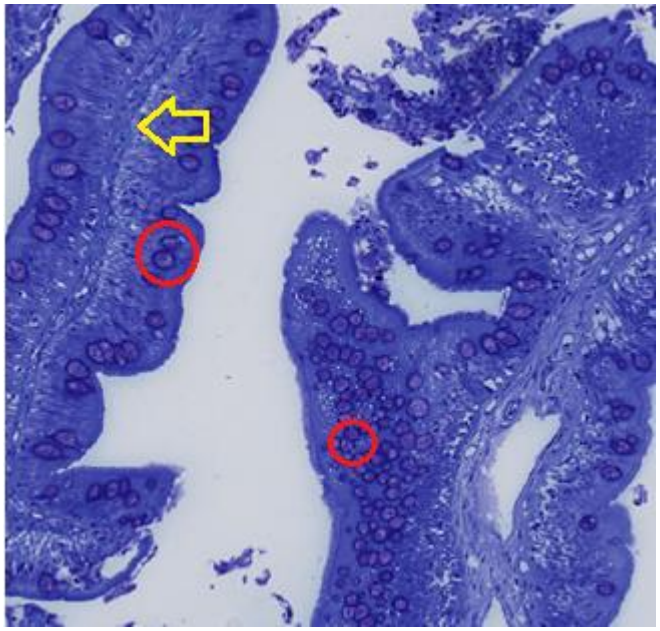

Figure 15. Mucus cells evaluated as large and evenly distributed (Score 5) highlighted with a red circle (Left side). The right side shows mucus cells evaluated as densely distributed and small (Score 1). The yellow arrow highlights the lamina propria, being evaluated as very thin (Score 1).

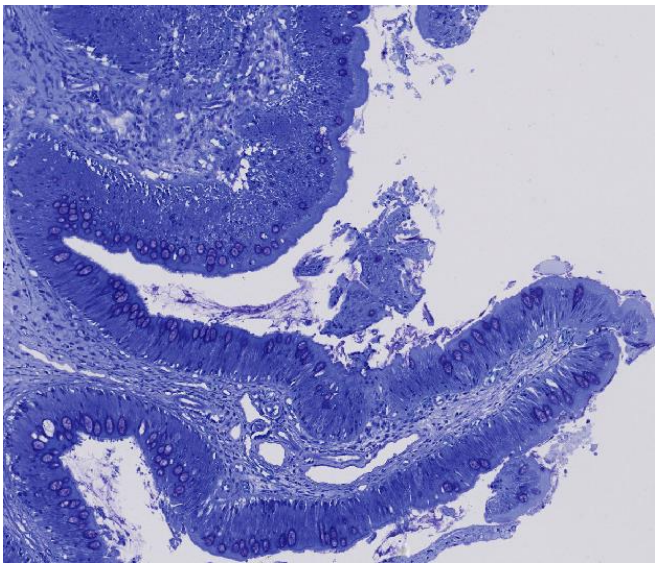

Figure 16. Mucus cells evaluated as a score 2, with both small and large. Lamina propria appearing as more distinct.

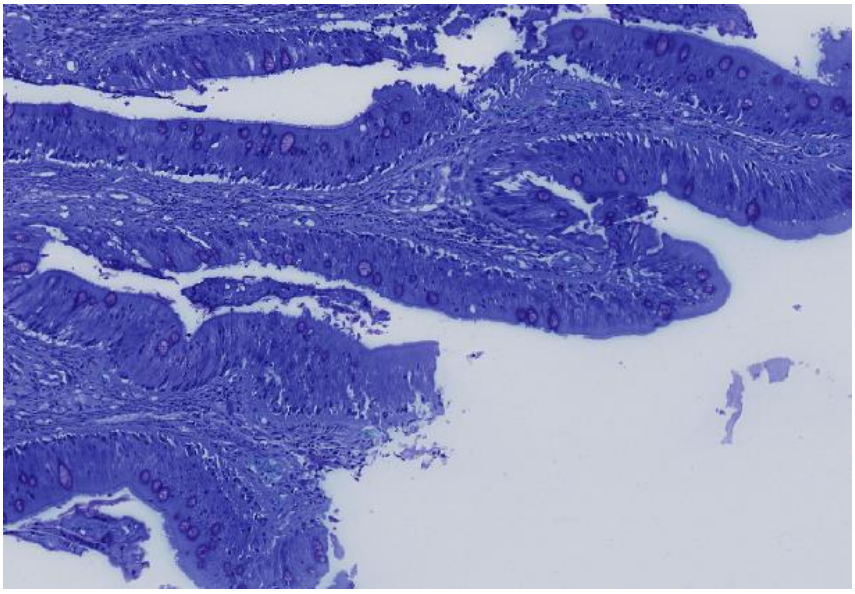

Figure 17. Mucus cells evaluated as a score 5, and lamina propria as more distinct. Sample showing varying degree of tissue damage to the villus and outer enterocyte layer.

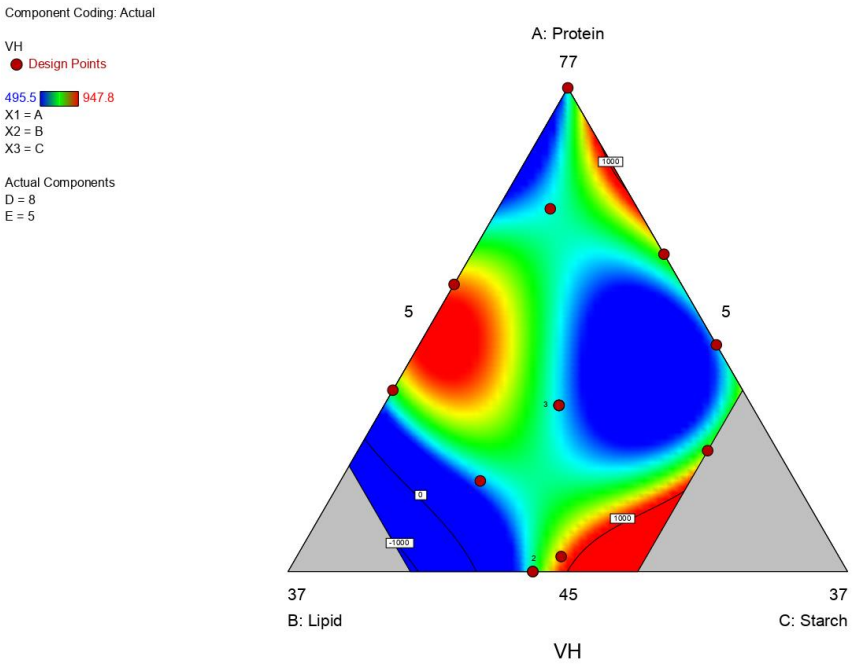

Figure 18. The average villus height from all visible villi presented in a color spectrum, where blue is the lowest value and red being the highest. The specific macronutrient composition of the diets represents a red dot in the triangular mixed design model, where the positioning in relation to point A (Protein), point B (Lipid) and point C (Starch) corresponds to the macronutrient content of the given diet. N=6 for each diet. P-value= 0,540

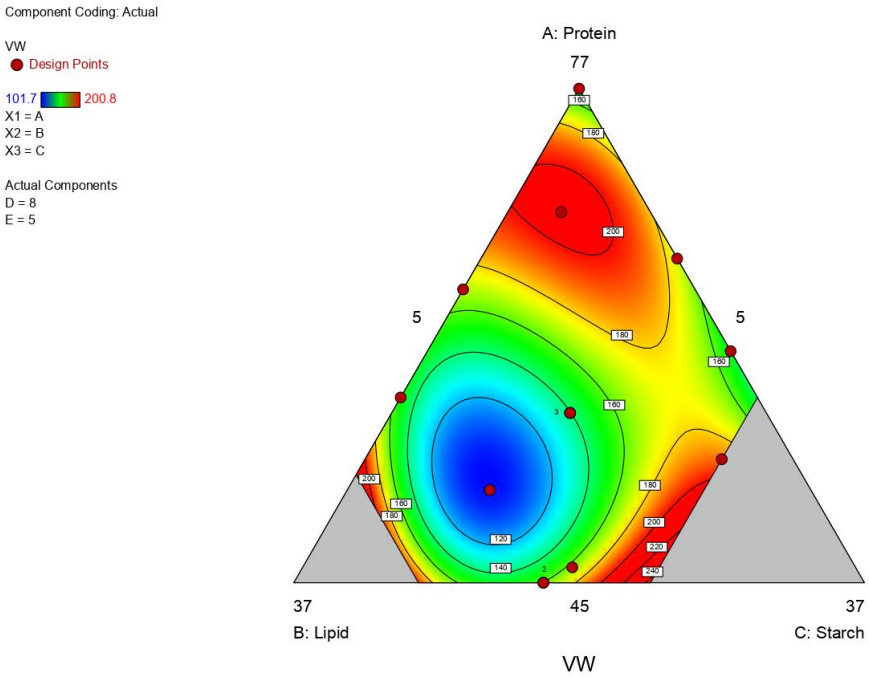

Figure 19. The average villus width from all visible villi presented in a color spectrum, where blue is the lowest value and red being the highest. The specific macronutrient composition of the diets represents a red dot in the triangular mixed design model, where the positioning in relation to point A (Protein), point B (Lipid) and point C (Starch) corresponds to the macronutrient content of the given diet. N=6 for each diet. P-value=0,446.

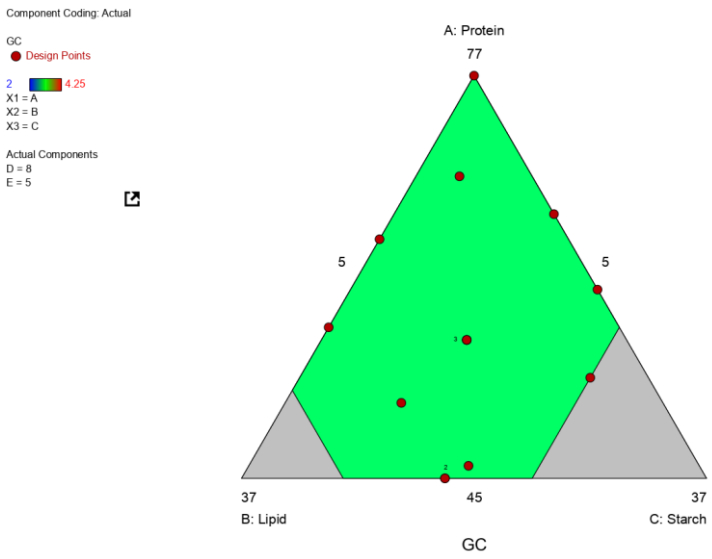

Figure 20. The average goblet cell score from all visible villi presented in a color spectrum, where blue is the lowest value and red being the highest. The specific macronutrient composition of the diets represents a red dot in the triangular mixed design model, where the positioning in relation to point A (Protein), point B (Lipid) and point C (Starch) corresponds to the macronutrient content of the given diet. N=6 per diet.

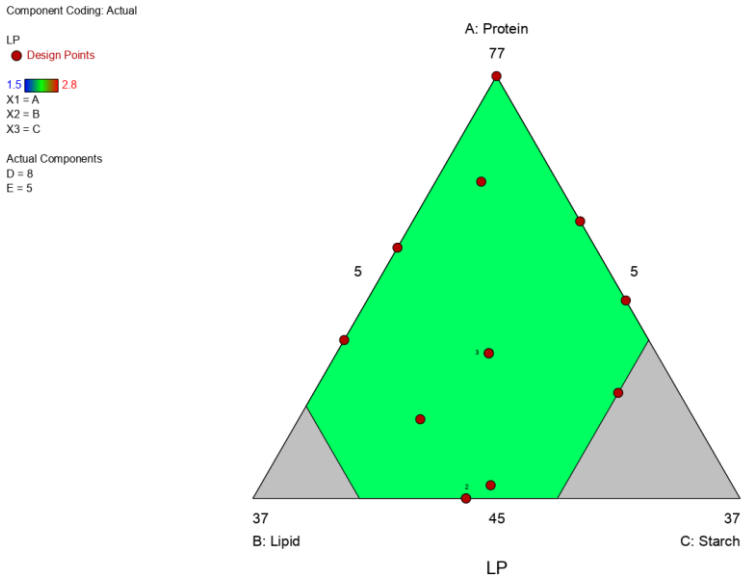

Figure 21. The average lamina propria score from all visible villi presented in a color spectrum, where blue is the lowest value and red being the highest. The specific macronutrient composition of the diets represents a red dot in the triangular mixed design model, where the positioning in relation to point A (Protein), point B (Lipid) and point C (Starch) corresponds to the macronutrient content of the given diet. N=6 per diet.

3.3- Gene expression

3.3.1- Interleukins

The gene expression patterns of interleukin 1b, IL6, IL11b and IL12b were low in most samples (Figure 22,23,24 and 25), with some individuals in several of the tanks having a higher expression pattern. The outliers showing elevated gene expression patterns across the different genes, most often occurred in the same individuals. Both tanks given diet 5 had an outlier in the expression of interleukin 1b, with a gene expression of above twice the amount relative to the housekeeping gene Ef1a1. Diet 11 had one sample with above 6 times the relative gene expression of IL1b, and 3 times the expression of IL6 and IL12b. Diet 6 had a sample with higher expressions of IL1b, IL12b and a 7-fold increase of IL6. Diet 10 had one sample with an 8-fold expression of IL6, where all the other genes showed low expression. Another sample in diet 10 had a 2-fold increase in IL1b and 4-fold expression of IL12b. Diet 2.1 had one sample with a 3-fold expression of IL6, and a 3-fold expression of IL12b.

The mean qPCR value for each gene depending on the diet, fitted unto the triangular mixed design model is shown in Figure 28,29,30,31,32 and 33. For interleukin 1b there is a trend towards elevated gene expression seen in diets high in lipids and carbohydrates with a p-value of 0,046. A similar effect was seen regarding interleukin 6 (Figure 23), where both high lipids and high carbohydrates has a higher gene expression. For interleukin 6 an area of higher protein inclusion also showed elevated gene expression results. ANOVA deemed this model as not significant due to a p-value of 0,284 (Appendix 2). For both mean values of interleukin 11b and interleukin 12b, no difference in expression was seen when fitted into the triangular design model considering macronutrient composition (Figure 30 and 31).

3.3.2- Igm and imuc

Immunoglobulin (IgM) was lowly expressed in most samples, with diet 9 and 5 having the highest mean expression (Figure 26). Intestinal mucin was highly expressed in diet 6 with a sample showing a 13-fold expression, as well as the mean being higher not including the outlier (Figure 27). Diet 10 and 11 had one sample each with a 4,4-fold and 5,8-fold expression respectively. The mean qPCR value for immunoglobulin shown in the triangular design model (Figure 32), shows the lowest values towards the higher concentrations of carbohydrates or lipids. The highest value was seen in the diets with the highest inclusion of protein. ANOVA deemed this model as not significant, with a p-value of 0,225 (Appendix 2).

For intestinal mucin (Figure 27) the highest mean expression was associated with high lipids, as well as higher starch inclusion (p-value=0,0297).

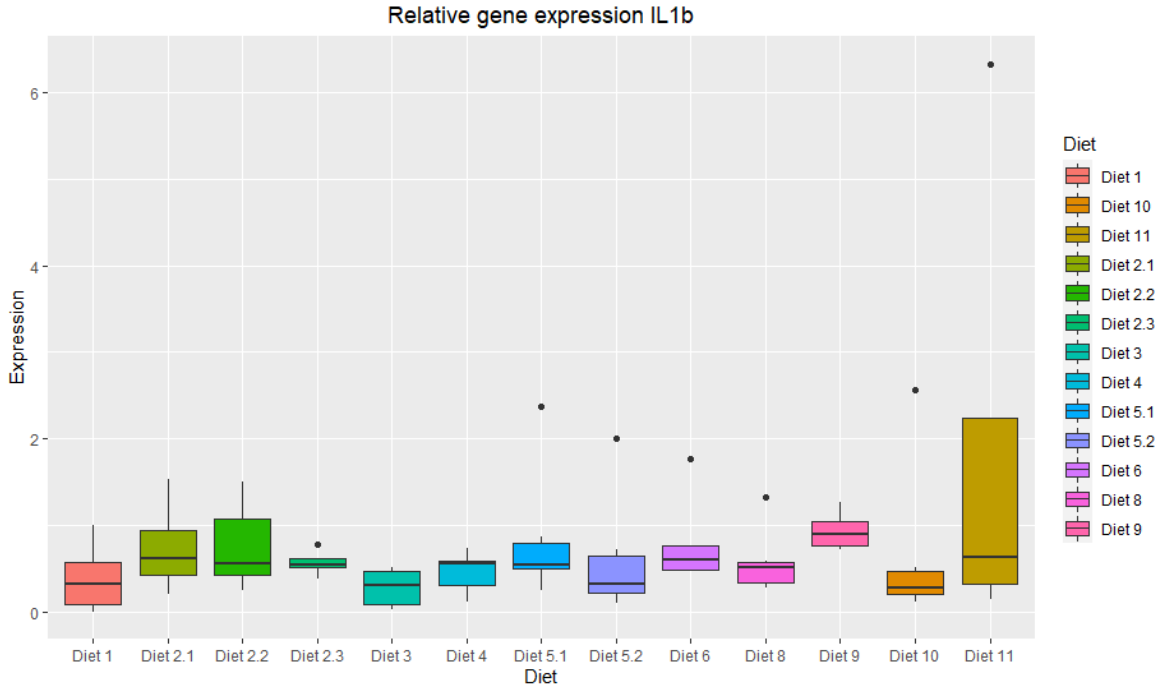

Figure 22. Relative gene expression of Interleukine 1b for each diet isolated from the distal intestine from Atlantic halibut, shown in relation to reference gene Ef1a1. Horizontal lines marks the mean value, vertical lines shows the standard deviation, and dots marks outliers. N=6 for each diet.

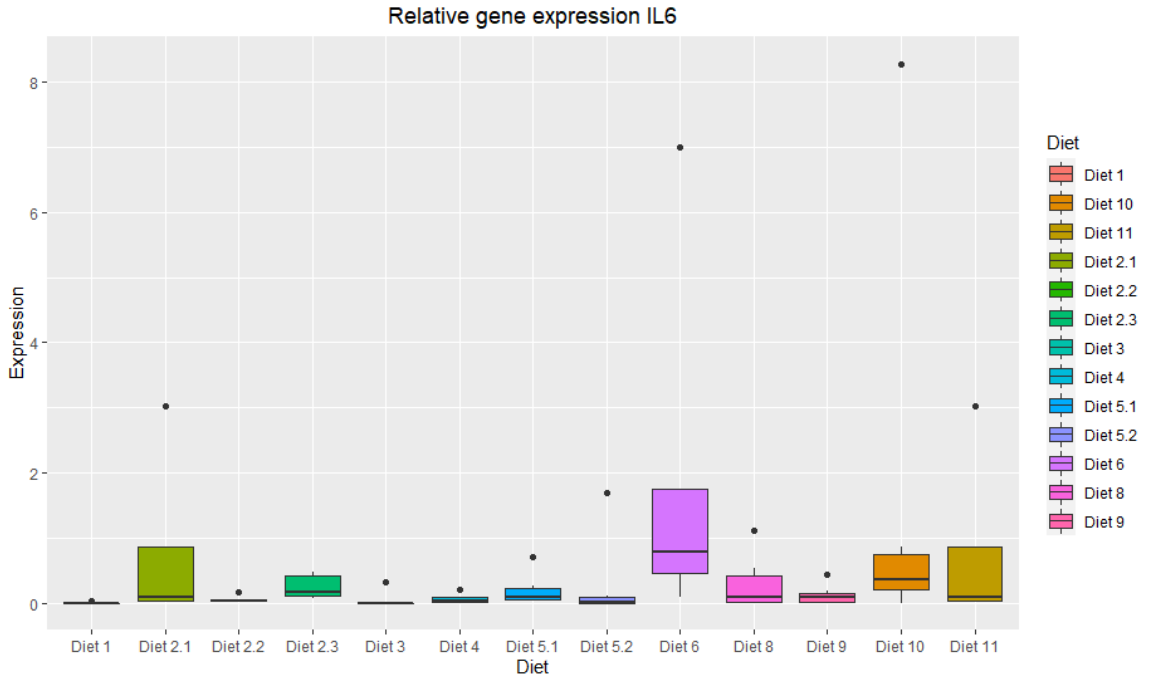

Figure 23. Relative gene expression of Interleukine 6 for each diet isolated from the distal intestine from Atlantic halibut, shown in relation to reference gene Ef1a1. Horizontal lines marks the mean value, vertical lines shows the standard deviation, and dots marks outliers. N=6 for each diet.

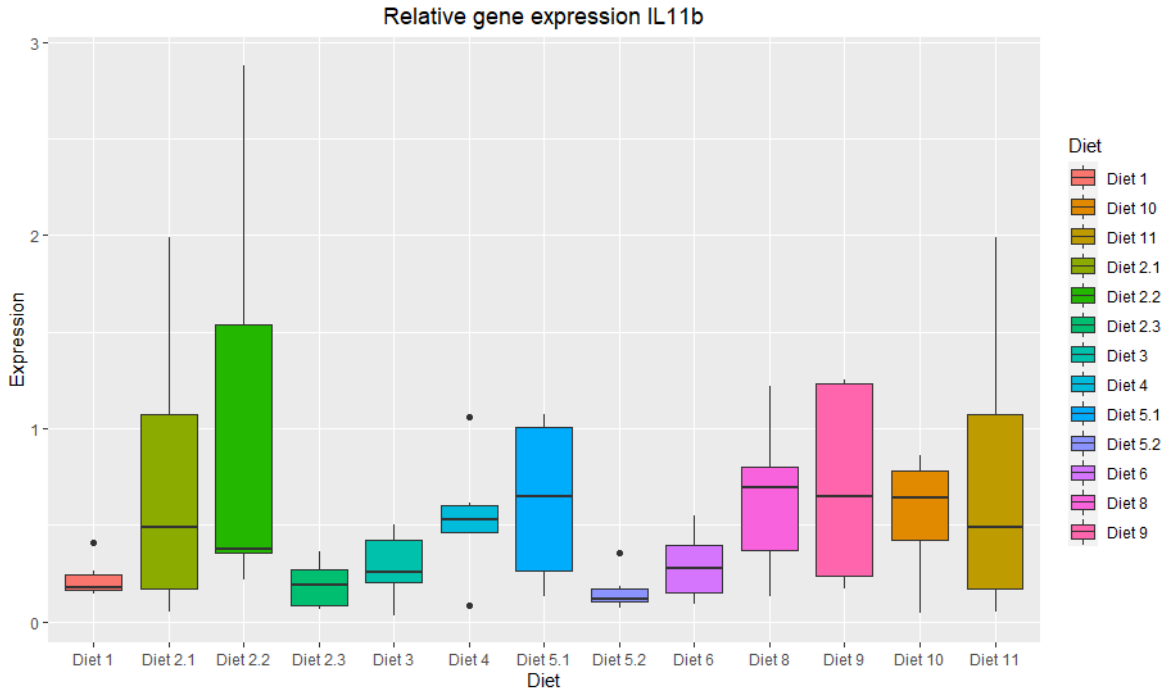

Figure 24. Relative gene expression of Interleukine 11b for each diet isolated from the distal intestine from Atlantic halibut, shown in relation to reference gene Ef1a1. Horizontal lines marks the mean value, vertical lines shows the standard deviation, and dots marks outliers. N=6 for each diet.

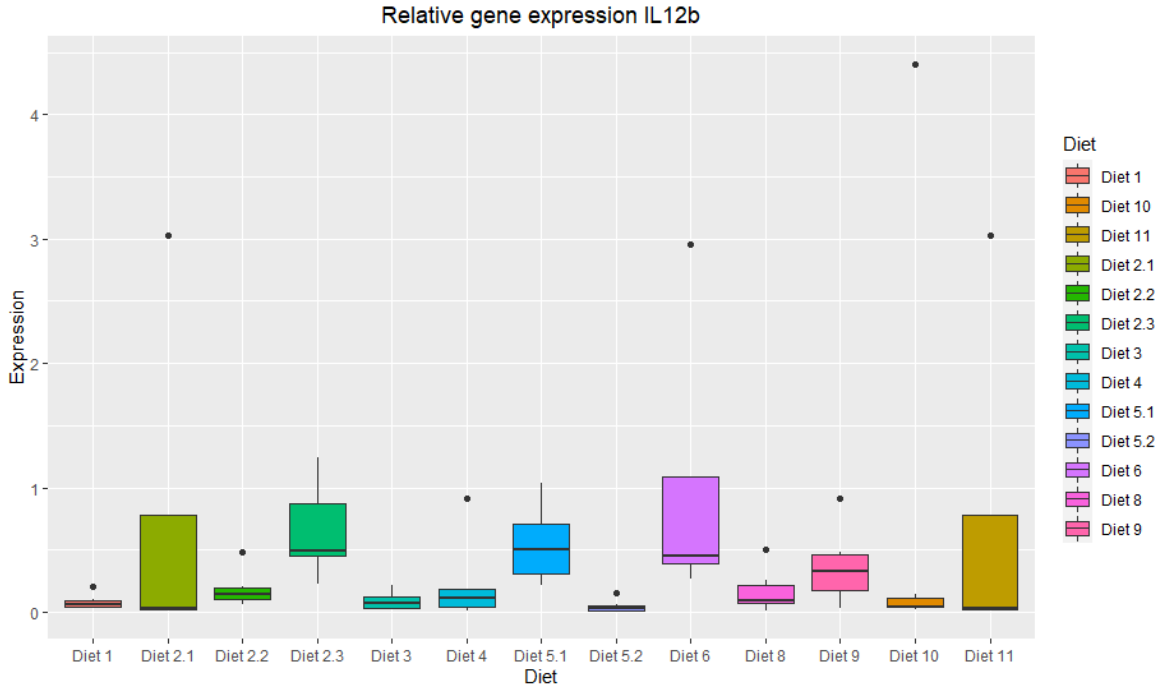

Figure 25. Relative gene expression of Interleukine 12b for each diet isolated from the distal intestine from Atlantic halibut, shown in relation to reference gene Ef1a1. Horizontal lines marks the mean value, vertical lines shows the standard deviation, and dots marks outliers. N=6 for each diet.

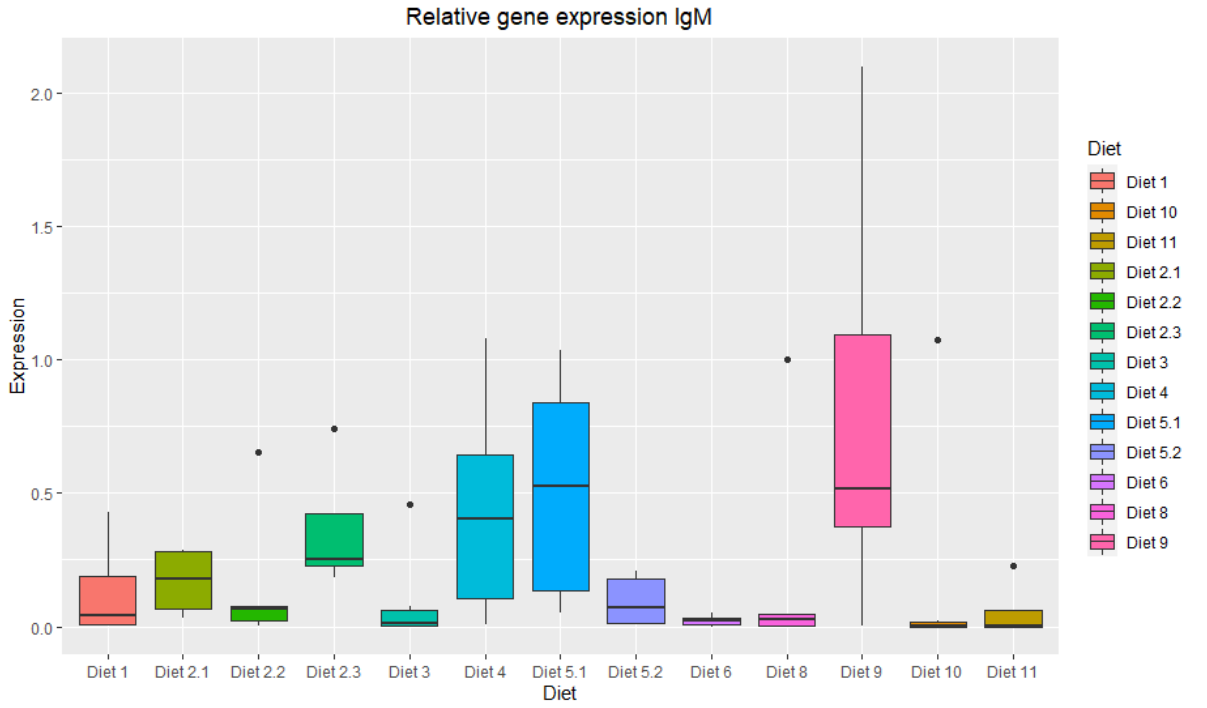

Figure 26. Relative gene expression of IgM for each diet isolated from the distal intestine from Atlantic halibut, shown in relation to reference gene Ef1a1. Horizontal lines marks the mean value, vertical lines shows the standard deviation, and dots marks outliers. N=6 for each diet.

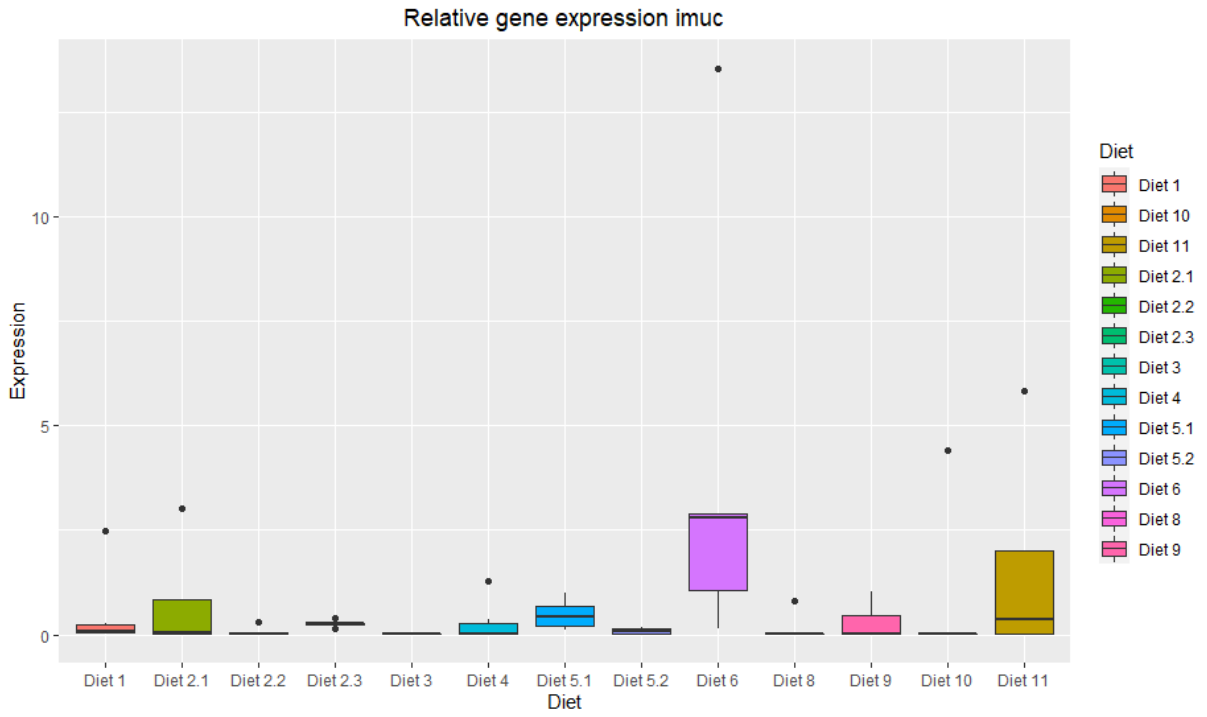

Figure 27. Relative gene expression of Intestinal mucin for each diet isolated from the distal intestine from Atlantic halibut, shown in relation to reference gene Ef1a1. Horizontal lines marks the mean value, vertical lines shows the standard deviation, and dots marks outliers. N=6 for each diet.

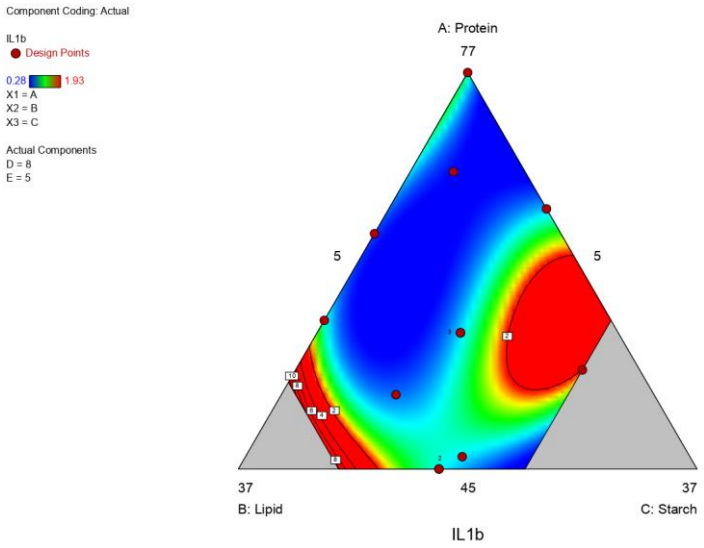

Figure 28. The average relative gene expression value of interleukin 1b visualized in a color spectrum, where blue is the lowest value and red being the highest. The specific macronutrient composition of the diets represents a red dot in the triangular mixed design model, where the positioning in relation to point A (Protein), point B (Lipid) and point C (Starch) corresponds to the macronutrient content of the given diet. P-value= 0,046. N=6 for each diet.

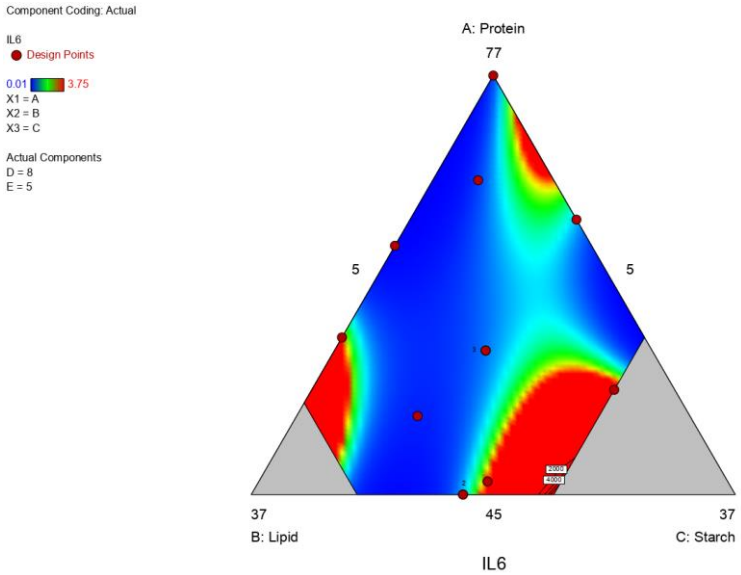

Figure 29. The average relative gene expression value of interleukin 6 visualized in a color spectrum, where blue is the lowest value and red being the highest. The specific macronutrient composition of the diets represents a red dot in the triangular mixed design model, where the positioning in relation to point A (Protein), point B (Lipid) and point C (Starch) corresponds to the macronutrient content of the given diet. P-value=0,284. N=6 for each diet.

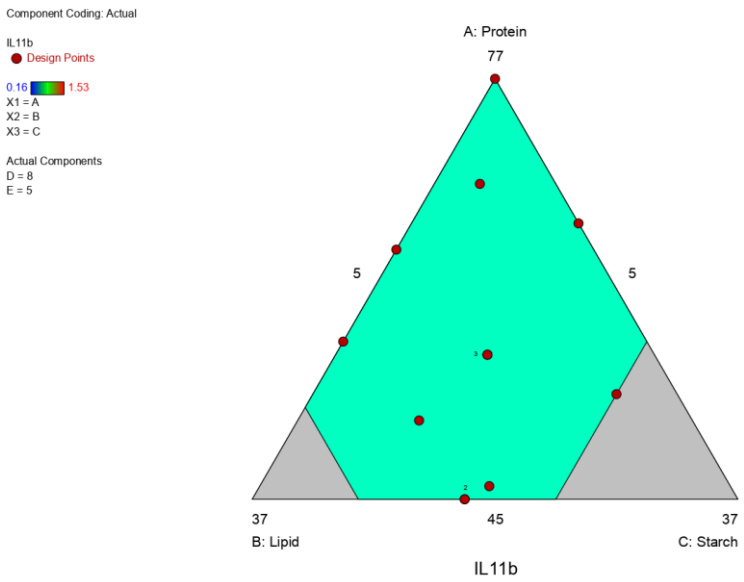

Figure 30. The average relative gene expression value of interleukin 11b visualized in a color spectrum, where blue is the lowest value and red being the highest. The specific macronutrient composition of the diets represents a red dot in the triangular mixed design model, where the positioning in relation to point A (Protein), point B (Lipid) and point C (Starch) corresponds to the macronutrient content of the given diet. N=6 for each diet.

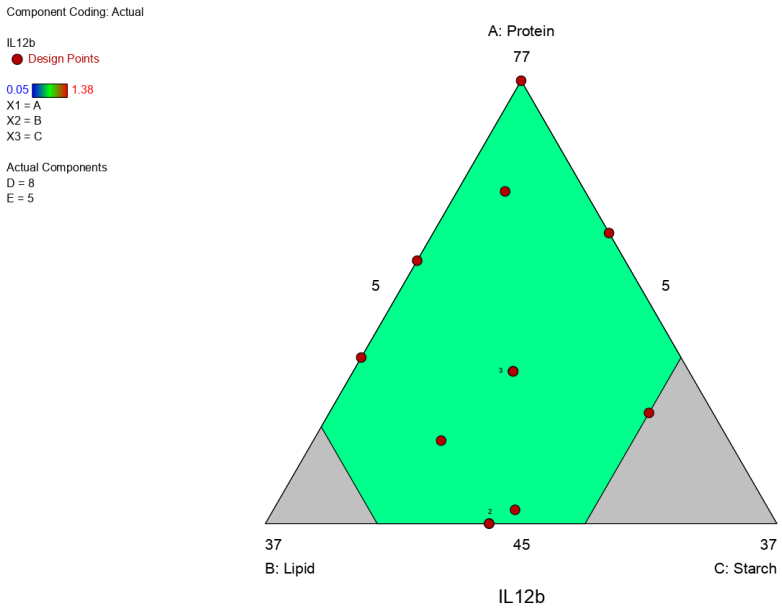

Figure 31. The average relative gene expression value of interleukin 12b visualized in a color spectrum, where blue is the lowest value and red being the highest. The specific macronutrient composition of the diets represents a red dot in the triangular mixed design model, where the positioning in relation to point A (Protein), point B (Lipid) and point C (Starch) corresponds to the macronutrient content of the given diet. N=6 for each diet.

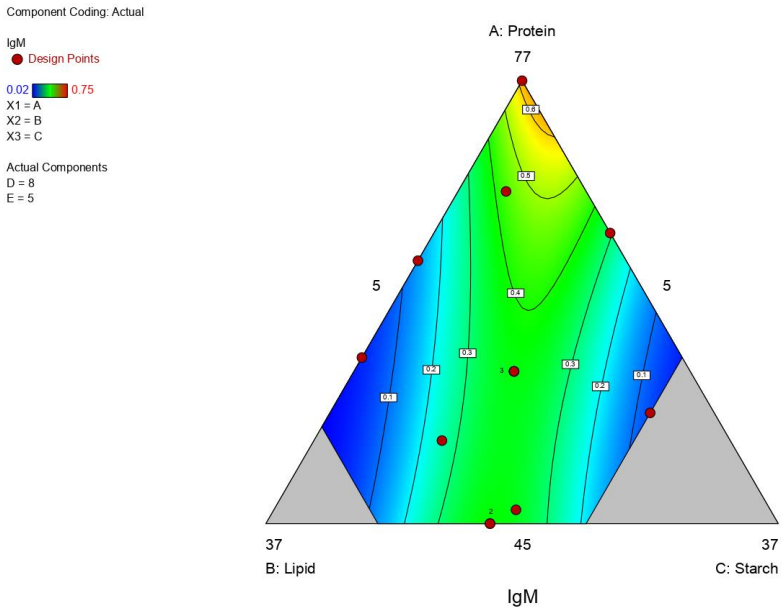

Figure 32. The average relative gene expression value of immunoglobulin visualized in a color spectrum, where blue is the lowest value and red being the highest. The specific macronutrient composition of the diets represents a red dot in the triangular mixed design model, where the positioning in relation to point A (Protein), point B (Lipid) and point C (Starch) corresponds to the macronutrient content of the given diet. P-value=0,225. N=6 for each diet.

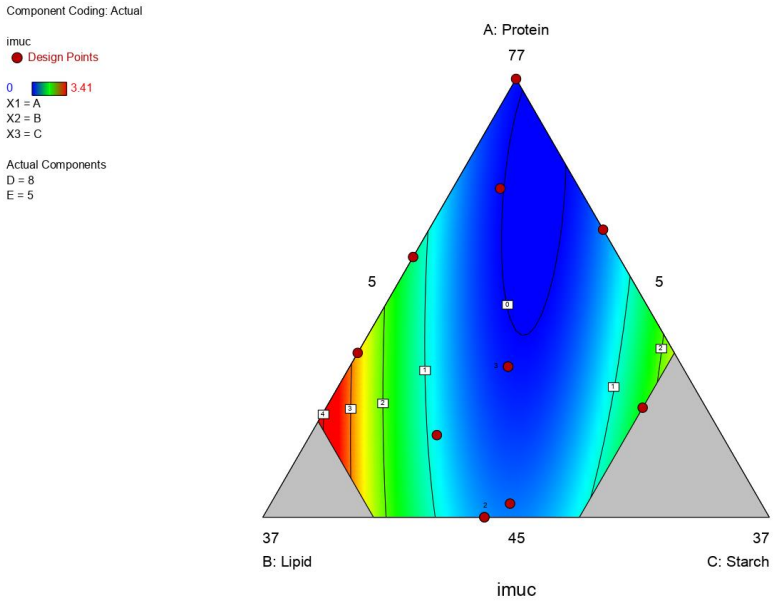

Figure 33. The average relative gene expression value of intestinal mucin visualized in a color spectrum, where blue is the lowest value and red being the highest. The specific macronutrient composition of the diets represents a red dot in the triangular mixed design model, where the positioning in relation to point A (Protein), point B (Lipid) and point C (Starch) corresponds to the macronutrient content of the given diet. P-value= 0,03. N=6 for each diet.

Discussion

4.1. Growth and performance

The highest growth in this trial was associated with higher lipid inclusion and lower protein, seen in Figure 8,9 and 10 and. When accounting for mean weight at the start of the trial, the effect of higher lipids is more pronounced as seen in Figure 10 visualizing the average specific growth rate. Lipid levels of up to 23% in this case, seemed to be an explanatory factor for high SGR (P-value of 0,0112). In Figure 9 visualizing mean end-point weight the model was deemed as not significant (P-value of 0,1227), even though the trend was similar. One problem with looking at SGR over end-point weight, is smaller fish having a higher expected growth rate. This could make the impression of a smaller group growing faster compared to a larger group. It could be argued that end point weight is better for assessing growth over such a long time period, but that exact starting weight should be taken into consideration. A similar effect could also be speculated to be the reason for the last SGR measurement yielding best growth with higher protein and starch, where the fish in the tanks given these diets were smaller on beforehand. The missing data from diet 6 and 5 should be considered when evaluating the growth, where only 26 and 31 measurements were included respectively due to the missing PIT registration data. These two diets were the best preforming ones as well according to the final weight model, which could be severely affected by the reduction in individuals used for the mean weight of these two diets.

One essential aspect that does not fit to this model, is diet 7 having to be euthanized during the experiment due to bad growth. Diet 7 containing 28% lipids, compared to 23% and 21% in the best preforming diets, causing such a rapid decline in growth is not consistent with previous research on halibut this size (Aksnes et al., 1996), (Hamre et al., 2005; Helland & Grisdale-Helland, 1998). Levels of up to 32,5% lipid inclusion had been used successfully previously, where increased dietary fat was associated with higher carcass lipid retention (Aksnes et al., 1996). A reduction in growth with lipids above 24% has been seen in juvenile halibut previously (Hamre et al., 2003; Hjertnes et al., 1993), where a 25% inclusion limit has been suggested. In juvenile halibut (0,4g) a higher mortality occurred with the highest levels of lipid inclusion of up to 30% (Hamre et al., 2005). This was hypothesized to be due to the high inclusion of soy lecithin, which has been linked to pathological effects in the enterocytes of turbot (*Scophthalmus maximus*) during start-feeding (Leifson et al., 2003). In this experiment marine lecithin was used, consisting of 9,3% of the dietary content in the highest

lipid diet. Marine lecithin has not been associated with pathological effect when used as a main source for phospholipid (Leifson et al., 2003).

Lower growth in the diets containing the highest level of protein, confirms the previous research suggesting the protein demand of halibut being lower than the highest values tested (Árnason et al., 2009; Helland & Grisdale-Helland, 1998). The lowest protein content which in this trial was 41% in diet 5, still seems to be over the minimum requirement for protein for halibut this size. Due to total energy content of the diet increasing with higher lipids, a protein sparing effect of lipids has previously been seen (Helland & Grisdale-Helland, 1998). In salmonids increased lipids at lower protein seems to better facilitate growth (Hillestad & Johnsen, 1994). According to previous research for halibut, a similar effect has not been found (Árnason et al., 2009; Hamre et al., 2005; Helland & Grisdale-Helland, 1998; Nortvedt, 1997). This effect is probably due to halibut reducing its feed intake, to compensate for the higher ingestion of total energy. More research to find the true minimum protein levels for larger halibut, could help determining how the protein requirements develop throughout the growth period. Through this additional feed cost savings from lower protein levels, combined with a good feeding regime would help getting the feed costs down additionally.

Carbohydrate content according to this study seemed to facilitate growth well, where diet 10 and 11 with 27% carbohydrates preformed the third and fourth best. Further analysis of digestibility and feed intake should be taken into consideration. In trout a negative correlation has been seen between increased starch content and digestibility (Spannhof & Plantikow, 1983). This could increase the amount of intestinal fluids as well as inhibiting starch hydrolysis, causing an increased passage of intestinal content thus reducing the available absorption-time. (Spannhof & Plantikow, 1983). Feed structure and performance is another aspect of consideration, where macronutrient differences could be reflected in how well the feed preforms due to structure. This could affect appetite and tank environment, which could result in differences between the tanks.

After the trial some fish screened positive for a viral disease, that was identified as a herpes-like virus infection. How much this has affected the fish during the experiment is hard to say, as this was only identified after the trial end. This could severely affect the tanks and have greater impacts on growth compared to an isolated macronutrient effect. The disease had not previously been identified in the IMR facility at Austevoll.

4.2. Histology

No obvious signs of inflammation or dietary effect was seen on the histological examinations. Villus height (Figure 18) shows higher carbohydrate inclusion diets, as being one of the areas in the triangular design model with the longest villi. A shorter area was seen towards higher lipid inclusion. This model was however regarded as not significant (p=0,54). If we were to expect an inflammatory response due to macronutrients, a shortening of villus is one of the known signs of dietary induced inflammation (Baeverfjord & Krogdahl, 1996). Long villi are associated with better nutrient absorption. a higher amount of enterocytes as well as higher enzyme production (Caspary, 1992). Villus width (Figure 19) appeared as wide towards higher carbohydrates, as well as towards higher protein. Although this model was deemed as not significant (p=0,46). Thinner villi have been recognized as an inflammatory response, where it can affect nutrient absorption capacity (Estruch et al., 2018). The fish having the thinnest villi in this trial according to Figure 19, was the higher lipid inclusion. Unfortunately, with the fish on the highest lipid diet being slaughtered before the trial end, no evaluation of histology was possible on this fish.

The evaluation of mucus cells did not show any trends regarding macronutrient composition as seen in Figure 20. The role of mucus cells is complex, where they play an active role in maintaining mucosal integrity and intestinal tract immunity. An inflammatory response in the gut could potentially be identified by the differentiation and development of mucus cells (Yang & Yu, 2021) . In salmon an acute response was identified for the mucus cells in the distal intestine, as a response to hypoxias stress (Djordjevic et al., 2021). If any of the diets in this trial would have caused a stress response within the distal intestine, we could expect to see this reflected in goblet cell count and composition. The lamina propria scores did not seem to be affected by macronutrient composition either according to Figure 21. No observation of a diet type correlation regarding the lamina propria appearance, further strengthens the notion of a wide tolerance level of macronutrients in halibut.

The dietary sensitivity to carbohydrates seen in juvenile halibut (Hamre et al., 2003), appeared not to affect halibut this size in a negative way both regarding growth and histological analysis. This was an expected result, where previous trials with halibut this size have not seen negative effects of increased carbohydrate levels (Árnason et al., 2009). The higher carbohydrate inclusion was mainly due to increased tapioca starch and wheat, which the halibut seemed to tolerate well. The ingredients used in this trial are mainly the

ingredients used in commercial feed production, where none of the single ingredients were expected to cause any issues in isolation.

A weakness in this histological study is the heterogeneity between the individual samples, regarding fixation angle and section quality. To best evaluate the different individuals, the hindgut sections should be equal to make valid comparisons. In this case there was a large discrepancy between the different samples in visibility due to angle, but also how successful the fixation was. Some samples had damages to the outer enterocyte layer, which could be mistaken for dietary induced lesions but was most likely due to unsuccessful fixation or rough handling. Prolonged dehydration in ethanol can cause tissues to shrink and get overhardened, causing morphological changes to the histological samples (Troiano et al., 2009), which could be a possible explanation for this.

4.3. Gene expression

The qPCR data for interleukin 1b (p=0,046) and interleukin 6 (p=0,284) showed a tendency for elevated expression towards a higher lipid and carbohydrate inclusion. IL1b is one of the most widely studied cytokines, and has been described in several teleost species (Øvergård et al., 2012). IL1b is recognized as one of the main mediators of inflammation, where it is involved in processes involving immune responses (Lu et al., 2008). An increase in expression for this gene could be seen as an important mediator for inducing several pleiotropic downstream responses, that are not always detectible when looking at other health parameters (Lu et al., 2008). IL6 is also one key mediators of the cytokine network, where it has an important role in both innate and adaptive immune responses (Castellana et al., 2008). Interestingly IL6 is reported to not be actively produced under normal circumstances, but rather rapidly upregulated as a response to pro-inflammatory molecules or pathogenic invasions (Castellana et al., 2008). The high expression in some of the samples should therefore arguably not be seen as a normal occurrence, but as an intestinal response to a potential stressor. Immunological mechanisms in need of a continuous energy supply, can over time lead to a chronic stress status affecting overall fish health (Estruch et al., 2018).

The expression of interleukin 11b and 12b (Figure 30 and 31) could not be predicted from a macronutrient compositional perspective. The relative expression of both were quite low compared to the other interleukins. Interleukin 11b has been identified with sharing similar properties to IL6, where it is involved in the formation of new blood cells and pleiotropic properties involving inflammatory processes (Øvergård et al., 2012). The kidneys was proposed as the main area of importance regarding the regulation of IL11b in halibut, but the

posterior gut showed a high level of transcript as well (Øvergård et al., 2012). Even though interleukin 12b had an overall low expression, there were a few outliers showing higher expression levels (Figure 31). Interleukin 12 is identified as a pro-inflammatory molecule similar to the other cytokines used in this trial, where it is recognized as critical in the defense against pathogens and intracellular bacteria (Nascimento et al., 2007). IL12b stimulates the activity of natural killer cells and T-cells, and is important for regulating the cellular immune response as seen in mammals (Øvergård et al., 2012).

Immunoglobulin (IgM) is produced from B cells, and is an antibody recognized as one of the most important for systemic immunity (Sunyer, 2012). How well IgM acts as a proxy for macronutrient tolerance might be argued, where it is most often associated with its phagocytosis capabilities for dealing with pathogens (Sunyer, 2012). The elevated gene expression of IgM seen in diet 9 ($p=0,225$), might reflect a bacterial or viral infection in the sampled fish. This should be taken into consideration when evaluating the growth results from the trial, where diet 9 was the diet with the highest protein content. Having underlying disease affecting this tank, could be an explanatory reason for the low growth results for this tank. IgT could have been another gene of interest to study, where it has been identified as an antibody with non-inflammatory properties involved in mucosal immunity (Sunyer, 2012). In rainbow trout B cells were found to either express IgM or IgT, where IgT was mostly found expressed in the gut (Zhang et al., 2010). This might have provided additional insight regarding the dietary effect on the mucosal response from the different ingredient compositions.

The elevated expression of intestinal mucin ($p<0,03$) associated with higher lipids in the diet, should be taken into consideration when evaluating the dietary effect seen from macronutrients. Mucins are a group of glycoproteins found in all wet surfaced epithelial tissues, where their activity is affected by a number of different stressors (Pérez-Sánchez et al., 2013). Intestinal mucin is a gene described several times in gilthead seabream (*Sparus aurata*), where its activity is proposed to be an important proxy for intestinal health due to its clear correlation to the nutritional background. The gene was found to be highly expressed in the posterior gut, where it was downregulated by a inclusion of vegetable oil and from parasitic infections (Pérez-Sánchez et al., 2013). The elevation of imuc in this case should not necessarily be regarded as a negative response, where it could also reflect a well-functioning intestinal integrity. In what way this gene regulates the intestinal integrity in halibut is a topic worth further research and discussion.

4.4. Future perspectives

For the future perspectives on this topic, finding a true minimum protein inclusion level should be of interest. Further research on the limits for carbohydrates and lipids in larger halibut would provide insightful for evaluating the possibilities of applicable macronutrient compositions. A similarly structured trial to this one using halibut with a higher starting weight, could reveal how the macronutrient needs develop as the fish grows. Knowledge regarding how plant ingredients affect halibut would also be of great utility, where this would help with feed associated costs and aspects of sustainability. Further determining what specific gene activity to look for as a proxy for intestinal health in halibut, could also help to evaluate the utility of different dietary compositions.

Conclusion

This thesis further strengthens the insight that a high protein inclusion in larger halibut does not necessarily yield the best growth. The four best preforming diets were below 57% protein, where the best growth was seen towards a higher inclusion of dietary lipids. The sharp reduction in growth seen in the diet containing 28% lipids, could provide caution against moving beyond 25%. Halibut this size appears to tolerate a carbohydrate content of up to 27% well from a growth perspective. Histological analysis of the distal intestine did not show any signs of a dietary effect on intestinal morphology or signs of inflammation. A dietary effect on the expression if IL1b and imuc in the intestine was seen from qPCR, with elevated levels towards higher lipids and carbohydrates. This could be an indicator of a possible inflammatory response from a dietary macronutrient higher in lipids and carbohydrates, which raises concerns regarding fish health and performance in the long run. The implication from these results further proves that a lower protein content in the diet of halibut in the on-growth stage, could be implemented without negatively affecting growth. This could be of economic impact, reducing the production cost associated with this species. However, without further knowledge regarding the long-term inflammatory effects and specific tolerance levels for dietary lipids and carbohydrates, potential changes should be implemented with caution.

References:

Aksnes, A., Hjertnes, T., & Opstvedt, J. (1996, 1996/10/15/). Effect of dietary protein level on growth and carcass composition in Atlantic halibut (Hippoglossus hippoglossus L). *Aquaculture, 145*(1), 225-233. https://doi.org/https://doi.org/10.1016/S0044-8486(96)01347-6

Árnason, J., Imsland, A. K., Gústavsson, A., Gunnarsson, S., Arnarson, I., Reynisson, H., Jónsson, A. F., Sráradóttir, H., & Thorarensen, H. (2009, 2009/06/16/). Optimum feed formulation for Atlantic halibut (Hippoglossus hippoglossus L.): Minimum protein content in diet for maximum growth. *Aquaculture, 291*(3), 188-191. https://doi.org/https://doi.org/10.1016/j.aquaculture.2009.03.025

Baeverfjord, G., & Krogdahl, A. (1996). Development and regression of soybean meal induced enteritis in Atlantic salmon, Salmo salar L., distal intestine: a comparison with the intestines of fasted fish. *Journal of Fish Diseases, 19*(5), 375-387. https://doi.org/https://doi.org/10.1046/j.1365-2761.1996.d01-92.x

Bakke-McKellep, A. M., Penn, M. H., Salas, P. M., Refstie, S., Sperstad, S., Landsverk, T., Ringø, E., & Krogdahl, Å. (2007). Effects of dietary soyabean meal, inulin and oxytetracycline on intestinal microbiota and epithelial cell stress, apoptosis and proliferation in the teleost Atlantic salmon (Salmo salar L.). *British Journal of Nutrition, 97*(4), 699-713. https://doi.org/10.1017/S0007114507381397

Bankhead, P., Loughrey, M. B., Fernández, J. A., Dombrowski, Y., McArt, D. G., Dunne, P. D., McQuaid, S., Gray, R. T., Murray, L. J., Coleman, H. G., James, J. A., Salto-Tellez, M., & Hamilton, P. W. (2017, 2017/12/04). QuPath: Open source software for digital pathology image analysis. *Scientific Reports, 7*(1), 16878. https://doi.org/10.1038/s41598-017-17204-5

Berge, G. M., Grisdale-Helland, B., & Helland, S. J. (1999, 1999/07/15/). Soy protein concentrate in diets for Atlantic halibut (Hippoglossus hippoglossus). *Aquaculture, 178*(1), 139-148. https://doi.org/https://doi.org/10.1016/S0044-8486(99)00127-1

Caspary, W. F. (1992). Physiology and pathophysiology of intestinal absorption. *The American Journal of Clinical Nutrition, 55*(1), 299S-308S. https://doi.org/10.1093/ajcn/55.1.299s

Castellana, B., Iliev, D. B., Sepulcre, M. P., MacKenzie, S., Goetz, F. W., Mulero, V., & Planas, J. V. (2008, 2008/07/01/). Molecular characterization of interleukin-6 in the gilthead seabream (Sparus aurata). *Molecular Immunology, 45*(12), 3363-3370. https://doi.org/https://doi.org/10.1016/j.molimm.2008.04.012

Chen, L., Feng, L., Jiang, W.-D., Jiang, J., Wu, P., Zhao, J., Kuang, S.-Y., Tang, L., Tang, W.-N., Zhang, Y.-A., Zhou, X.-Q., & Liu, Y. (2015, 2015/11/01/). Intestinal immune function, antioxidant status and tight junction proteins mRNA expression in young grass carp (Ctenopharyngodon idella) fed riboflavin deficient diet. *Fish & Shellfish Immunology, 47*(1), 470-484. https://doi.org/https://doi.org/10.1016/j.fsi.2015.09.037

Cornell, J. (2011). The Original Mixture Problem: Designs and Models for Exploring the Entire Simplex Factor Space. In (pp. 23-93). https://doi.org/10.1002/9780470907443.ch2

Djordjevic, B., Morales-Lange, B., McLean Press, C., Olson, J., Lagos, L., Mercado, L., & Øverland, M. (2021, Jan 21). Comparison of Circulating Markers and Mucosal Immune Parameters from Skin and Distal Intestine of Atlantic Salmon in Two Models of Acute Stress. *Int J Mol Sci, 22*(3). https://doi.org/10.3390/ijms22031028

Egerton, S., Wan, A., Murphy, K., Collins, F., Ahern, G., Sugrue, I., Busca, K., Egan, F., Muller, N., Whooley, J., McGinnity, P., Culloty, S., Ross, R. P., & Stanton, C. (2020, 2020/03/06). Replacing fishmeal with plant protein in Atlantic salmon (Salmo salar) diets by supplementation with fish protein hydrolysate. *Scientific Reports, 10*(1), 4194. https://doi.org/10.1038/s41598-020-60325-7

Estruch, G., Collado, M. C., Monge-Ortiz, R., Tomás-Vidal, A., Jover-Cerdá, M., Peñaranda, D. S., Pérez Martínez, G., & Martínez-Llorens, S. (2018, 2018/10/03). Long-term feeding with high plant protein based diets in gilthead seabream (Sparus aurata, L.) leads to changes in the inflammatory and immune related gene expression at intestinal level. *BMC Veterinary Research, 14*(1), 302. https://doi.org/10.1186/s12917-018-1626-6

Gallardo, P., Bueno, G. W., Araneda, C., & Benfey, T. (2022, 2022/02/01/). Status of Atlantic halibut (Hippoglossus hippoglossus) aquaculture production technology in Chile. *Aquaculture Reports, 22*, 100958. https://doi.org/https://doi.org/10.1016/j.aqrep.2021.100958

Garrido, S., Ben-Hamadou, R., Santos, A. M. P., Ferreira, S., Teodósio, M. A., Cotano, U., Irigoien, X., Peck, M. A., Saiz, E., & Ré, P. (2015, 2015/11/24). Born small, die young: Intrinsic, size-selective mortality in marine larval fish. *Scientific Reports, 5*(1), 17065. https://doi.org/10.1038/srep17065

Grisdale-Helland, B., HELLAND, S. J., BAEVERFJORD, G., & BERGE, G. M. (2002). Full-fat soybean meal in diets for Atlantic halibut: growth, metabolism and intestinal histology. *Aquaculture Nutrition, 8*(4), 265-270. https://doi.org/https://doi.org/10.1046/j.1365-2095.2002.00216.x

Hamre, K., Baeverfjord, G., & Harboe, T. (2005, 2005/02/28/). Macronutrient composition of formulated diets for Atlantic halibut (Hippoglossus hippoglossus, L.) juveniles, II: protein/lipid levels at low carbohydrate. *Aquaculture, 244*(1), 283-291. https://doi.org/https://doi.org/10.1016/j.aquaculture.2004.12.007

Hamre, K., Øfsti, A., Næss, T., Nortvedt, R., & Holm, J. C. (2003, 2003/11/10/). Macronutrient composition of formulated diets for Atlantic halibut (Hippoglossus hippoglossus, L.) juveniles. *Aquaculture, 227*(1), 233-244. https://doi.org/https://doi.org/10.1016/S0044-8486(03)00506-4

Hatlen, B., Grisdale-Helland, B., & Helland, S. J. (2005, 2005/09/12/). Growth, feed utilization and body composition in two size groups of Atlantic halibut (Hippoglossus hippoglossus) fed diets

differing in protein and carbohydrate content. *Aquaculture, 249*(1), 401-408. https://doi.org/https://doi.org/10.1016/j.aquaculture.2005.03.040

Haug, T. (1990). Biology of the Atlantic Halibut, Hippoglossus hippoglossus (L., 1758). In J. H. S. Blaxter & A. J. Southward (Eds.), *Advances in Marine Biology* (Vol. 26, pp. 1-70). Academic Press. https://doi.org/https://doi.org/10.1016/S0065-2881(08)60198-4

Haug, T., & Gulliksen, B. (1988, 1988/12/22). Fecundity and oocyte sizes in ovaries of female Atlantic halibut, Hippoglossus hippoglossus (L.). *Sarsia, 73*(4), 259-261. https://doi.org/10.1080/00364827.1988.10413411

Haug, T., & Tjemsland, J. (1986, 1986/07/01/). Changes in size- and age-distributions and age at sexual maturity in atlantic halibut, Hippoglossus hippoglossus, caught in North Norwegian waters. *Fisheries Research, 4*(2), 145-155. https://doi.org/https://doi.org/10.1016/0165-7836(86)90039-1

Helland, S. J., & Grisdale-Helland, B. (1998, 1998/07/01/). Growth, feed utilization and body composition of juvenile Atlantic halibut (Hippoglossus hippoglossus) fed diets differing in the ratio between the macronutrients. *Aquaculture, 166*(1), 49-56. https://doi.org/https://doi.org/10.1016/S0044-8486(98)00273-7

Hillestad, M., & Johnsen, F. (1994, 1994/07/01/). High-energy/low-protein diets for Atlantic salmon: effects on growth, nutrient retention and slaughter quality. *Aquaculture, 124*(1), 109-116. https://doi.org/https://doi.org/10.1016/0044-8486(94)90366-2

Hjertnes, T., Gulbrandsen, K., Johnsen, F., & Opstvedt, J. (1993). Effect of dietary protein, carbohydrate and fat levels in dry feed for juvenile halibut (Hippoglossus hippoglossus L.). *Colloques de l'INRA (France)*.

Krogdahl, A., Bakke-McKellep, A., Roed, K., & Baeverfjord, G. (2000). Feeding Atlantic salmon Salmo salar L. soybean products: effects on disease resistance (furunculosis), and lysozyme and IgM levels in the intestinal mucosa. *Aquaculture Nutrition, 6*(2), 77-84.

Leifson, R. M., Homme, J. M., Lie, ø., Myklebust, R., & Strøm, T. (2003). Three different lipid sources in formulated start-feeds for turbot (Scophthalmus maximus, L.) larvae – effect on growth and mitochondrial alteration in enterocytes. *Aquaculture Nutrition, 9*(1), 33-42. https://doi.org/https://doi.org/10.1046/j.1365-2095.2003.00225.x

Lu, D.-Q., Bei, J.-X., Feng, L.-N., Zhang, Y., Liu, X.-C., Wang, L., Chen, J.-L., & Lin, H.-R. (2008, 2008/02/01/). Interleukin-1β gene in orange-spotted grouper, Epinephelus coioides: Molecular cloning, expression, biological activities and signal transduction. *Molecular Immunology, 45*(4), 857-867. https://doi.org/https://doi.org/10.1016/j.molimm.2007.08.009

Mangor-Jensen, A., Harboe, T., Shields, R. J., Gara, B., & Naas, K. E. (1998). Atlantic halibut, Hippoglossus hippoglossus L., larvae cultivation literature, including a bibliography.

Aquaculture Research, 29(12), 857-886. https://doi.org/https://doi.org/10.1046/j.1365-2109.1998.29120857.x

Martins, D. A., Valente, L. M. P., & Lall, S. P. (2007, 2007/03/06/). Effects of dietary lipid level on growth and lipid utilization by juvenile Atlantic halibut (Hippoglossus hippoglossus, L.). *Aquaculture, 263*(1), 150-158. https://doi.org/https://doi.org/10.1016/j.aquaculture.2006.10.017

Murray, H. M., Lall, S. P., Rajaselvam, R., Boutilier, L. A., Blanchard, B., Flight, R. M., Colombo, S., Mohindra, V., & Douglas, S. E. (2010, 2010/01/07/). A nutrigenomic analysis of intestinal response to partial soybean meal replacement in diets for juvenile Atlantic halibut, Hippoglossus hippoglossus, L. *Aquaculture, 298*(3), 282-293. https://doi.org/https://doi.org/10.1016/j.aquaculture.2009.11.001

Nascimento, D. S., Vale, A. d., Tomás, A. M., Zou, J., Secombes, C. J., & dos Santos, N. M. S. (2007, 2007/03/01/). Cloning, promoter analysis and expression in response to bacterial exposure of sea bass (Dicentrarchus labrax L.) interleukin-12 p40 and p35 subunits. *Molecular Immunology, 44*(9), 2277-2291. https://doi.org/https://doi.org/10.1016/j.molimm.2006.11.006

Nimalan, N., Sørensen, S. L., Fečkaninová, A., Koščová, J., Mudroňová, D., Gancarčíková, S., Vatsos, I. N., Bisa, S., Kiron, V., & Sørensen, M. (2022, 2022/01/30/). Mucosal barrier status in Atlantic salmon fed marine or plant-based diets supplemented with probiotics. *Aquaculture, 547*, 737516. https://doi.org/https://doi.org/10.1016/j.aquaculture.2021.737516

Nortvedt, R. (1997). *multivariate approach to the study of growth, feed utilization, body composition and sensory assessment of cultured Atlantic halibut (Hippoglossus hippoglossus, L., 1758)*. Dept. of Fisheries and Marine Biology, University of Bergen, 1997.

Ottesen, O. H., Babiak, I., & Dahle, G. (2009, 2009/01/17/). Sperm competition and fertilization success of Atlantic halibut (Hippoglossus hippoglossus L.). *Aquaculture, 286*(3), 240-245. https://doi.org/https://doi.org/10.1016/j.aquaculture.2008.09.018

Pérez-Sánchez, J., Estensoro, I., Redondo, M. J., Calduch-Giner, J. A., Kaushik, S., & Sitjà-Bobadilla, A. (2013). Mucins as Diagnostic and Prognostic Biomarkers in a Fish-Parasite Model: Transcriptional and Functional Analysis. *PLOS ONE, 8*(6), e65457. https://doi.org/10.1371/journal.pone.0065457

Sahlmann, C., Sutherland, B. J. G., Kortner, T. M., Koop, B. F., Krogdahl, Å., & Bakke, A. M. (2013, 2013/02/01/). Early response of gene expression in the distal intestine of Atlantic salmon (Salmo salar L.) during the development of soybean meal induced enteritis. *Fish & Shellfish Immunology, 34*(2), 599-609. https://doi.org/https://doi.org/10.1016/j.fsi.2012.11.031

Secombes, C. J., Wang, T., & Bird, S. (2011, 2011/12/01/). The interleukins of fish. *Developmental & Comparative Immunology, 35*(12), 1336-1345. https://doi.org/https://doi.org/10.1016/j.dci.2011.05.001

Silva, P. F., McGurk, C., Knudsen, D. L., Adams, A., Thompson, K. D., & Bron, J. E. (2015, 2015/08/01/). Histological evaluation of soya bean-induced enteritis in Atlantic salmon (Salmo salar L.): Quantitative image analysis vs. semi-quantitative visual scoring. *Aquaculture, 445*, 42-56. https://doi.org/https://doi.org/10.1016/j.aquaculture.2015.04.002

Spannhof, L., & Plantikow, H. (1983, 1983/01/01/). Studies on carbohydrate digestion in rainbow trout. *Aquaculture, 30*(1), 95-108. https://doi.org/https://doi.org/10.1016/0044-8486(83)90155-2

Sunyer, J. O. (2012, Jun). Evolutionary and functional relationships of B cells from fish and mammals: insights into their novel roles in phagocytosis and presentation of particulate antigen. *Infect Disord Drug Targets, 12*(3), 200-212. https://doi.org/10.2174/187152612800564419

Troiano, N. W., Ciovacco, W. A., & Kacena, M. A. (2009, Mar 1). The Effects of Fixation and Dehydration on the Histological Quality of Undecalcified Murine Bone Specimens Embedded in Methylmethacrylate. *J Histotechnol, 32*(1), 27-31. https://doi.org/10.1179/his.2009.32.1.27

Wilson, M. R., & Warr, G. W. (1992, 1992/01/01/). Fish immunoglobulins and the genes that encode them. *Annual Review of Fish Diseases, 2*, 201-221. https://doi.org/https://doi.org/10.1016/0959-8030(92)90064-5

Yang, S., & Yu, M. (2021). Role of Goblet Cells in Intestinal Barrier and Mucosal Immunity. *J Inflamm Res, 14*, 3171-3183. https://doi.org/10.2147/jir.S318327

Yu, Y., Wang, Q., Huang, Z., Ding, L., & Xu, Z. (2020, 2020-October-02). Immunoglobulins, Mucosal Immunity and Vaccination in Teleost Fish [Review]. *Frontiers in Immunology, 11*. https://doi.org/10.3389/fimmu.2020.567941

Zhang, Y.-A., Salinas, I., Li, J., Parra, D., Bjork, S., Xu, Z., LaPatra, S. E., Bartholomew, J., & Sunyer, J. O. (2010, 2010/09/01). IgT, a primitive immunoglobulin class specialized in mucosal immunity. *Nature Immunology, 11*(9), 827-835. https://doi.org/10.1038/ni.1913

Øvergård, A.-C., Nepstad, I., Nerland, A. H., & Patel, S. (2012, 2012/03/01). Characterisation and expression analysis of the Atlantic halibut (Hippoglossus hippoglossus L.) cytokines: IL-1β, IL-6, IL-11, IL-12β and IFNγ. *Molecular Biology Reports, 39*(3), 2201-2213. https://doi.org/10.1007/s11033-011-0969-x

Øvergård, A.-C., Nerland, A. H., & Patel, S. (2010, 2010/05/11). Evaluation of potential reference genes for real time RT-PCR studies in Atlantic halibut (Hippoglossus Hippoglossus L.); during development, in tissues of healthy and NNV-injected fish, and in anterior kidney leucocytes. *BMC Molecular Biology, 11*(1), 36. https://doi.org/10.1186/1471-2199-11-36

Appendix 1- Ingredients list

Diet	1	2	3	4	5	6	7	8	9	10	11	12
	%	%	%	%	%	%	%	%	%	%	%	%
Fish meal	59,1	50,5	63,3	46,0	40,2	52,9	45,7	60,9	71,6	41,7	48,7	55,5
Wheat gluten	15,0	12,8	16,1	11,7	10,2	13,4	11,6	15,5	18,2	10,6	12,4	14,1
Wheat	9,5	14,1	9,3	15,1	15,6	9,3	13,2	3,8	2,8	9,0	4,4	1,4
Tapioca starch		8,4	3,3	5,4	12,1			16,3	4,0	23,4	26,5	24,9
Fish oil	8,0	7,2	3,0	11,5	11,7	12,8	15,6	0,2		7,5	3,1	0,5
Marine lecithin	4,6	4,0	1,8	6,5	6,6	6,9	9,3	0,2		4,2	1,8	0,4
NaH2PO4	1,4	1,3	1,2	1,5	1,4	1,9	1,7	1,3	1,3	1,5	1,5	1,5
CaCO3	0,5			0,5	0,5	0,9	1,0			0,4		
Stay-C	0,1	0,1	0,1	0,1	0,1	0,1	0,1	0,1	0,1	0,1	0,1	0,1
Vitamin mix	0,5	0,5	0,5	0,5	0,5	0,5	0,5	0,5	0,5	0,5	0,5	0,5
Mineral mix	0,5	0,5	0,5	0,5	0,5	0,5	0,5	0,5	0,5	0,5	0,5	0,5
Lys	0,5	0,5	0,6	0,5	0,4	0,5	0,5	0,5	0,6	0,4	0,4	0,5
Thr	0,3	0,2	0,3	0,2	0,2	0,2	0,2	0,2	0,3	0,2	0,2	0,2
Met	0,1		0,1	0,1		0,1	0,1		0,1			
His	0,1	0,1	0,2	0,1	0,1	0,1	0,1	0,1	0,2	0,1	0,1	0,1
Yttrium oxide	0,0	0,0	0,0	0,0	0,0	0,0	0,0	0,0	0,0	0,0	0,0	0,0
sum	100	100	100	100	100	100	100	100	100	100	100	100
Total P (%) dm	2	2	2	2	2	2	2	2	2	2	2	2
Soluble P (%) dm	0,8	0,8	0,8	0,8	0,8	1,0	0,9	0,8	0,8	0,8	0,8	0,8
Ca (%)	2	2	2	2	2	2	2	2	3	2	2	2
Ca/P (1.1)	1,2	1,1	1,2	1,1	1,1	1,2	1,2	1,2	1,2	1,1	1,1	1,1
Phospholipids (%lipids)	15	15	15	15	15	15	15	15	15	15	15	15
Starch	5	15	8	13	19	5	7	16	5	25	25	22
ω3 (%lipid)	19	18	18	19	19	19	19	18	18	19	18	18
lys (g/100 protein)	7,0	7,0	7,0	7,0	6,9	7,0	7,0	7,0	7,0	6,9	7,0	7,0
meth (g/100 protein)	2,5	2,4	2,5	2,5	2,4	2,5	2,5	2,4	2,5	2,4	2,4	2,5
thr (g/100 protein)	3,8	3,8	3,8	3,8	3,8	3,8	3,8	3,8	3,8	3,8	3,8	3,8
His (g/100 protein)	2,1	2,1	2,1	2,1	2,1	2,1	2,1	2,1	2,1	2,1	2,1	2,1
trp (g/100 protein)	0,8	0,8	0,8	0,8	0,8	0,8	0,8	0,8	0,8	0,8	0,8	0,8
Arg (g/100 protein)	5,7	5,7	5,7	5,6	5,6	5,7	5,6	5,7	5,7	5,7	5,7	5,7
Ile (g/100 protein)	3,7	3,7	3,7	3,7	3,7	3,7	3,7	3,7	3,7	3,7	3,7	3,7
Leu (g/100 protein)	6,4	6,4	6,4	6,4	6,4	6,4	6,4	6,4	6,4	6,4	6,4	6,4
Val (g/100 protein)	4,3	4,3	4,3	4,3	4,3	4,3	4,3	4,3	4,3	4,3	4,3	4,3
Composition on a wet basis												
Protein	59	51	63	47	42	53	47	60	71	42	48	55
Lipid	17	15	9	21	21	23	28	5	5	15	8	5
Carbohydrate	7	18	10	16	22	7	10	17	6	27	27	23
Ash	9	8	9	8	7	10	9	9	10	8	8	9
Water	7	8	8	7	8	7	7	9	8	8	9	9

Appendix 2-Model ANOVA

Response 1: SGR1

Source	Sum of Squares	df	Mean Square	F-value	p-value
Model	0.0219	9	0.0024	4.96	0.0462 significant
[(1)]Linear Mixture	0.0010	2	0.0005	1.01	0.4293
AB	0.0078	1	0.0078	15.92	0.0104
AC	0.0010	1	0.0010	2.10	0.2067
BC	0.0000	1	0.0000	0.0309	0.8674
ABC	0.0002	1	0.0002	0.4817	0.5186
AB(A-B)	0.0059	1	0.0059	11.99	0.0180
AC(A-C)	0.0021	1	0.0021	4.36	0.0911
BC(B-C)	0.0004	1	0.0004	0.8678	0.3943
Residual	0.0025	5	0.0005		
Lack of Fit	0.0009	2	0.0005	0.9006	0.4939 not significant
Pure Error	0.0015	3	0.0005		
Cor Total	0.0244	14			

Response 2: SGR2

Source	Sum of Squares	df	Mean Square	F-value	p-value
Model	0.0310	9	0.0034	1.16	0.4582 not significant
[(1)]Linear Mixture	0.0058	2	0.0029	0.9696	0.4407
AB	0.0063	1	0.0063	2.11	0.2063
AC	0.0016	1	0.0016	0.5298	0.4993
BC	0.0001	1	0.0001	0.0272	0.8755
ABC	6.920E-09	1	6.920E-09	2.333E-06	0.9988
AB(A-B)	0.0101	1	0.0101	3.41	0.1243
AC(A-C)	0.0010	1	0.0010	0.3308	0.5901
BC(B-C)	0.0002	1	0.0002	0.0507	0.8308

Residual	0.0148	5	0.0030		
Lack of Fit	0.0017	2	0.0009	0.1993	0.8294 not significant
Pure Error	0.0131	3	0.0044		
Cor Total	0.0458	14			

Response 3: SGR3

Source	Sum of Squares	df	Mean Square	F-value	p-value
Model	0.0309	9	0.0034	4.86	0.0711 not significant
[(1)]Linear Mixture	0.0073	2	0.0036	5.15	0.0782
AB	0.0036	1	0.0036	5.04	0.0881
AC	6.124E-06	1	6.124E-06	0.0087	0.9303
BC	0.0065	1	0.0065	9.16	0.0389
ABC	0.0066	1	0.0066	9.31	0.0380
AB(A-B)	0.0047	1	0.0047	6.62	0.0617
AC(A-C)	1.800E-06	1	1.800E-06	0.0025	0.9621
BC(B-C)	0.0000	1	0.0000	0.0365	0.8579
Residual	0.0028	4	0.0007		
Lack of Fit	0.0019	1	0.0019	6.59	0.0828 not significant
Pure Error	0.0009	3	0.0003		
Cor Total	0.0337	13			

Response 4: SGR4

Source	Sum of Squares	df	Mean Square	F-value	p-value
Model	0.0211	2	0.0106	5.65	0.0205 significant
[(1)]Linear Mixture	0.0211	2	0.0106	5.65	0.0205
Residual	0.0205	11	0.0019		
Lack of Fit	0.0165	8	0.0021	1.55	0.3936 not significant
Pure Error	0.0040	3	0.0013		

Cor Total	0.0417	13			

Response 5: Weight Nov 22

Source	Sum of Squares	df	Mean Square	F-value	p-value
Model	46546.84	2	23273.42	2.68	0.1127 not significant
[1]Linear Mixture	46546.84	2	23273.42	2.68	0.1127
Residual	95550.97	11	8686.45		
Lack of Fit	71451.11	8	8931.39	1.11	0.5174 not significant
Pure Error	24099.86	3	8033.29		
Cor Total	1.421E+05	13			

Response 6: SGR

Source	Sum of Squares	df	Mean Square	F-value	p-value
Model	0.0079	2	0.0040	6.94	0.0112 significant
[1]Linear Mixture	0.0079	2	0.0040	6.94	0.0112
Residual	0.0063	11	0.0006		
Lack of Fit	0.0054	8	0.0007	2.21	0.2767 not significant
Pure Error	0.0009	3	0.0003		
Cor Total	0.0142	13			

Response 7: IL1b

Source	Sum of Squares	df	Mean Square	F-value	p-value
Model	2.51	9	0.2789	9.36	0.0461 significant
[1]Linear Mixture	0.7003	2	0.3502	11.75	0.0381
AB	0.1517	1	0.1517	5.09	0.1093
AC	0.1517	1	0.1517	5.09	0.1093
BC	0.0615	1	0.0615	2.06	0.2464
ABC	0.0637	1	0.0637	2.14	0.2400
AB(A-B)	0.0732	1	0.0732	2.46	0.2151

AC(A-C)	0.2059	1	0.2059	6.91	0.0784
BC(B-C)	0.2134	1	0.2134	7.16	0.0753
Pure Error	0.0894	3	0.0298		
Cor Total	2.60	12			

Response 8: IL6

Source	Sum of Squares	df	Mean Square	F-value	p-value	
Model	29.24	9	3.25	2.16	0.2842	not significant
[(1)]Linear Mixture	10.16	2	5.08	3.39	0.1701	
AB	0.4324	1	0.4324	0.2881	0.6287	
AC	0.1805	1	0.1805	0.1203	0.7516	
BC	1.51	1	1.51	1.00	0.3901	
ABC	2.04	1	2.04	1.36	0.3281	
AB(A-B)	0.0015	1	0.0015	0.0010	0.9765	
AC(A-C)	0.4089	1	0.4089	0.2725	0.6378	
BC(B-C)	0.8744	1	0.8744	0.5826	0.5008	
Pure Error	4.50	3	1.50			
Cor Total	33.74	12				

Response 9: IL11b

Source	Sum of Squares	df	Mean Square	F-value	p-value	
Model	0.0000	0				
Residual	5.90	12	0.4913			
Lack of Fit	2.37	9	0.2635	0.2243	0.9649	not significant
Pure Error	3.52	3	1.17			
Cor Total	5.90	12				

Response 10: IL12b

Source	Sum of Squares	df	Mean Square	F-value	p-value
Model	0.0000	0			
Residual	12.46	12	1.04		
Lack of Fit	8.42	9	0.9350	0.6941	0.7056 not significant
Pure Error	4.04	3	1.35		
Cor Total	12.46	12			

Response 11: IgM

Source	Sum of Squares	df	Mean Square	F-value	p-value
Model	1.33	5	0.2655	1.84	0.2245 not significant
[(1)]Linear Mixture	0.0884	2	0.0442	0.3055	0.7461
AB	0.0084	1	0.0084	0.0582	0.8163
AC	0.1814	1	0.1814	1.25	0.2996
BC	0.7748	1	0.7748	5.36	0.0538
Residual	1.01	7	0.1446		
Lack of Fit	0.6142	4	0.1535	1.16	0.4709 not significant
Pure Error	0.3979	3	0.1326		
Cor Total	2.34	12			

Response 12: imuc

Source	Sum of Squares	df	Mean Square	F-value	p-value
Model	8.12	5	1.62	4.94	0.0297 significant
[(1)]Linear Mixture	1.22	2	0.6106	1.86	0.2256
AB	0.5550	1	0.5550	1.69	0.2352
AC	1.26	1	1.26	3.83	0.0912
BC	5.74	1	5.74	17.45	0.0042

Residual	2.30	7	0.3290		
Lack of Fit	1.95	4	0.4887	4.21	0.1338 not significant
Pure Error	0.3485	3	0.1162		
Cor Total	10.43	12			

Response 13: VH

Source	Sum of Squares	df	Mean Square	F-value	p-value
Model	1.576E+05	9	17507.34	1.01	0.5395 not significant
[(1)]Linear Mixture	3491.72	2	1745.86	0.1008	0.9064
AB	55390.18	1	55390.18	3.20	0.1483
AC	28389.67	1	28389.67	1.64	0.2697
BC	1748.78	1	1748.78	0.1010	0.7666
ABC	24004.33	1	24004.33	1.39	0.3044
AB(A-B)	46639.54	1	46639.54	2.69	0.1762
AC(A-C)	34217.53	1	34217.53	1.98	0.2326
BC(B-C)	20169.39	1	20169.39	1.16	0.3413
Residual	69289.04	4	17322.26		
Lack of Fit	11819.33	1	11819.33	0.6170	0.4895 not significant
Pure Error	57469.70	3	19156.57		
Cor Total	2.269E+05	13			

Response 14: VW

Source	Sum of Squares	df	Mean Square	F-value	p-value
Model	7970.67	9	885.63	1.25	0.4459 not significant
[(1)]Linear Mixture	805.24	2	402.62	0.5676	0.6067
AB	170.89	1	170.89	0.2409	0.6492
AC	15.05	1	15.05	0.0212	0.8912
BC	480.86	1	480.86	0.6780	0.4566

ABC	195.31	1	195.31	0.2754	0.6275
AB(A-B)	373.33	1	373.33	0.5263	0.5083
AC(A-C)	72.49	1	72.49	0.1022	0.7652
BC(B-C)	204.00	1	204.00	0.2876	0.6202
Residual	2837.12	4	709.28		
Lack of Fit	126.53	1	126.53	0.1400	0.7331 not significant
Pure Error	2710.59	3	903.53		
Cor Total	10807.79	13			

Response 15: GC

Source	Sum of Squares	df	Mean Square	F-value	p-value
Model	0.0000	0			
Residual	4.93	13	0.3794		
Lack of Fit	3.64	10	0.3641	0.8456	0.6351 not significant
Pure Error	1.29	3	0.4306		
Cor Total	4.93	13			

Response 16: LP

Source	Sum of Squares	df	Mean Square	F-value	p-value
Model	0.0000	0			
Residual	1.57	13	0.1205		
Lack of Fit	0.7397	10	0.0740	0.2684	0.9506 not significant
Pure Error	0.8267	3	0.2756		
Cor Total	1.57	13			